AQUAPORIN 4 AND KIR4.1 DISTRIBUTION IN RETINAL GLIAL CELLS OF NORMAL MACAQUE EYES AND EYES WITH EXPERIMENTAL GLAUCOMA

By

Yanzhao Wang, B.S. Med.

THESIS

In partial satisfaction of the requirements for the degree of

MASTER OF SCIENCE
in
PHYSIOLOGICAL OPTICS

Presented to the Graduate Faculty of the

College of Optometry
University of Houston

December 2015

Approved:

_____
Laura J. Frishman, Ph.D. (Co-Chair)

_____
Louvenia Carter-Dawson, Ph.D. (Co-Chair)

_____
Nimesh B. Patel, O.D., Ph.D.

Committee in charge

Acknowledgments

I have been through the most important three years of my life at the University of Houston, Collage of Optometry with wonderful people working on this amazing research project. The journey was fill with difficulties, happiness, opportunities, challenges, but I enjoyed it all the way and I am proud of the outcome.

First, I would like to express my sincere gratitude to my advisor Professor Laura Frishman for her continuous support of my research, her patience, motivation, enthusiasm, and immense knowledge of the subject. Her guidance helped me throughout the entire time of my research. In particular, I am grateful for her enlightening me at the very first glance of my research. I am so appreciate that every letter she sent to me when I faced different challenges and keep asking me to be better. I could not have imagined having a better advisor and mentor for my graduate study.

My sincere appreciation also goes to Professor Louvenia Carter-Dawson, for teaching me how to design and perform experiments as well as demonstrating to me various lab techniques and methods. She was always there during the process of my thesis, providing valuable advice and suggestions. I really enjoyed working with her. Her constant guidance and support from the beginning to the final phase of the project enabled me to develop a thorough understanding of the research subject.

Besides my advisors, special thanks go to another thesis committee member, Professor Nimesh Patel, for his encouragement, insightful comments, and diligent questions.

Additionally, I would like to offer my best regards and blessings to all of those who assisted me in any respect during the completion of my thesis.

Finally, I would like to thank my parents Ping Wang and Juan Du, for their faith in me and allowing me to pursue this advanced degree abroad. I could not have made this far without their unconditional love and care since the day I was born.

List of Figures

List of Tables

Abstract

Purpose: The goal of the study was to determine the distribution of aquaporin 4 (AQP4) and a potassium inward rectifying channel (Kir4.1) in the Müller glia and astrocytes of the normal macaque monkey retina and to see how the distribution changed in eyes with experimental glaucoma.

Methods: Five Rhesus macaque monkeys, ranging in age from 7 to 11 years, had experimental glaucoma induced in one eye by argon laser scarification of the drainage angle to restrict the outflow of aqueous humor from the anterior chamber; the fellow eye served as a control. Posterior segments from the experimental glaucoma and fellow control eyes were fixed in 4% paraformaldehyde with phosphate buffer. Retina samples were taken from several nerve fiber rich regions within 5 mm of the optic nerve head (ONH) in the vicinity of the standard optical coherence tomography (OCT) peripapillary scan. Samples were cut at a thickness of 40 µm on a vibratome and were subjected to antigen retrieval followed by exposure to a polyclonal antibody to AQP4, or to Kir4.1, a monoclonal antibody to glutamine synthetase (GS, a marker for Müller cells), and a polyclonal antibody to glial fibrillary acidic protein (GFAP, a marker for astrocytes and reactive Müller cells). Antibody binding in retina was visualized with the appropriate secondary antibody conjugate of fluorescein, Cy3 and Cy5. Images of immunolabeled retina were captured by confocal microscopy.

Results: In the retinas of control eyes, AQP4 immunolabeling was present in GS positive Müller cell processes most prominently in the outer plexiform layer (OPL), around blood vessels, their trunks surrounding the nerve fiber bundles, and vitreal endfeet. AQP4 labeling co-localized to a lesser extent with the GFAP positive astrocytes of the retinal nerve fiber layer (RNFL). However, in eyes with experimental glaucoma and RNFL loss,

AQP4 was greatly reduced in Müller cells, whereas strong labeling was detected in GFAP positive astrocytes. AQP4 positive astrocyte processes aggregated in the region typically occupied by RNFL bundles and remained surrounded by Müller cell processes. In the retinas of control eyes, Kir4.1 immunolabeling was observed in Müller cells from OPL to RNFL, and was most prominent in the Müller cell processes in the OPL, the trunks surrounding nerve fiber bundles and processes around the blood vessels. Kir4.1 labeling in experimental eyes was similar to that in control eyes, except in the eyes with the severest loss of nerve bundles, where it aggregated in the region of the nerve fiber bundles.

Conclusions: In control eyes, AQP4 and Kir4 immunolabeling in the retina show a regional distribution similar to that described previously in rodents. The reduction of AQP4 in Müller cells of eyes with experimental glaucoma might impact water flux, particularly in inner retina. The increased presence of AQP4 in astrocytes of experimental eyes is a pathophysiological alteration that might reflect a compensation for the loss of AQP4 mediated water movement, or other changes in neighboring Müller cells and degenerating nerve fibers. The effects of experimental glaucoma on Kir4.1 channels were less obvious.

Chapter 1

General Introduction

Glaucoma is a leading cause of irreversible blindness worldwide in the elderly. It is a group of diseases characterized by progressive optic neuropathy and retinal ganglion cell loss with early damage to axons within the optic nerve head. There is increasing evidence that glial cells in the retina and optic nerve head are altered in glaucoma and that they are involved in the pathogenesis of disease. The retina, as a part of the central nervous system (CNS), contains two major types of glial cells: the macroglia, i.e. Müller glia (Müller cells) and astrocytes, and the microglia. Müller cells are unique to the retina, whereas astrocytes and microglia exist in retina and optic nerve and throughout the CNS as well. Microglia are the immune cells of the CNS. Beyond the lamina cribrosa of the optic nerve head, the myelin sheath of the optic nerve is composed of another macroglial cell, the oligodendrocyte. Glial cells provide protection for retinal neurons, as well as other neurons of the CNS and are responsible for maintaining retinal microenvironment and ion-water homeostasis. The present study is focused on the expression of two critical channels that reside in the plasma membranes of retinal macroglia: a water channel, Aquaporin 4 (AQP4), and an inward rectifying (ir) potassium channel, Kir4.1, both in normal eyes and eyes with glaucoma.

Aquaporin 4

AQP4 belongs to the large family of aquaporins that are integral membrane proteins that provide pathways for water into and out of cells. The family of aquaporins in mammals includes thirteen known protein subtypes: AQPs 0, 1, 2, 4, and 5 are classic water-selective aquaporins, while AQPs 3, 7, 9 and 10 are both water and glycerol selective, and are also called “aquaglyceroporins”, AQPs 6, 8, 11, and 12 are unorthodox aquaporins[1]. AQP1 was discovered by Peter Agre in 1991, and he was awarded the Nobel

Prize in Chemistry in 2003 for the discovery of water channels. Many of the aquaporins are expressed in the human eye: AQP0 is a major intrinsic protein (MIP) in lens fiber cells[2]; AQP1 is in the cornea endothelium, lens epithelium, ciliary epithelium, trabecular meshwork, and retinal pigment epithelium[2, 3]; AQP3 is in the corneal and conjunctival epithelia[3]; AQP4 is in the ciliary epithelium and retinal Müller glia[2]; AQP5 is in the corneal and lacrimal gland epithelia[3]; and AQP9 is in the retinal ganglion cells[3]. (Fig 1-1)

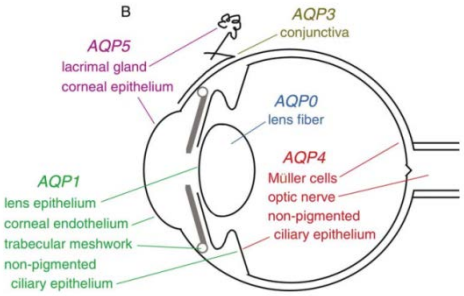

Figure 1-1 Sites of AQP water channel expression in ocular tissues[4]

The various aquaporins in the eye have functions that include maintaining transparency of the lens and cornea, and normal secretion of aqueous humor. In the retina they help to maintain cellular homeostasis and signal transduction[1]. Other studies have implicated aquaporins in other functions including angiogenesis, cell migration, tumor metastasis, wound healing, and even differentiation[5, 6]. A role for aquaporins has been suggested for certain ocular disorders such as bullous keratopathy, keratoconus[7], and Fuchs' dystrophy[8]. For the present study, we sought evidence that AQP4 has a role in experimental glaucoma in primates.

AQP4 serves as a classic water-selective channel in the CNS. For example, in cerebral edema, fluid enters or is eliminated from the CNS through AQP4 channels in astrocyte foot processes in the perivascular and subpial areas of the brain[9]. Also AQP4 has a proposed role in neuroexcitation and astrocyte migration[9]. Water movement through

AQP4 can result in contraction of the extracellular space (ECS) volume, causing increased ECS K^+ concentration, which facilitates uptake of K^+ by astrocytes and contributes to lamellipodial extension[9].

In ocular tissue in rodents, AQP4 is expressed in non-pigmented ciliary epithelium, in the Müller cells, whose cell bodies are in the inner nuclear layer (INL) of the retina, and fibrous astrocytes located in the optic nerve[10] (Fig 1-1, Fig 1-2). AQP4 is expressed more in the endfeet membrane domains than in other regions of the membranes. This polarized expression of AQP4 reflects the direction of water flux, and is similar to the polarized distribution of K^+ channels in the Müller glia. Indeed, AQP4 is largely co-localized with Kir4.1, a channel that mediates K^+ spatial buffering by the Müller cells. The two channels are involved in rapid water and potassium fluxes[11] and they work together to facilitate water transport across membranes when there are differences in osmotic gradients or hydrostatic pressure inside and outside of cells.

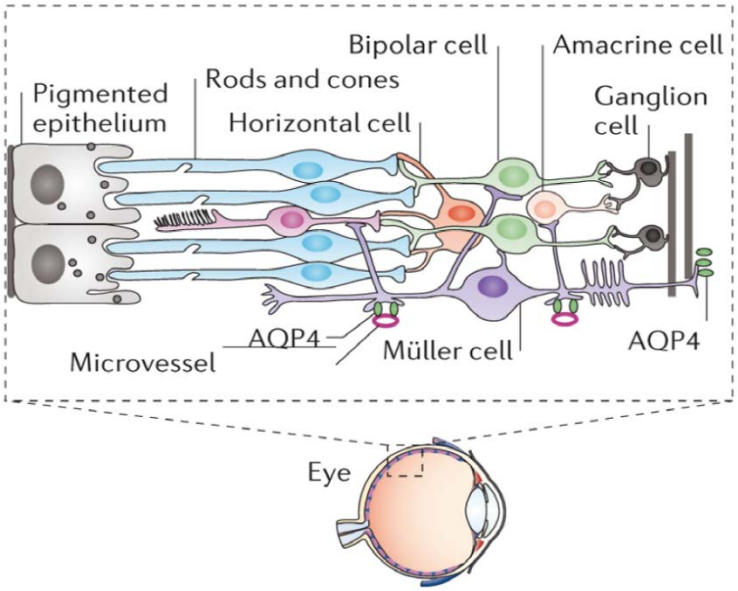

Figure 1-2 AQP4 expression in the retina. In the rat retina, AQP4 (green dots) is expressed in the perivascular processes and endfeet of Müller cells[9].

There is evidence that AQP4 plays a role in the pathogenesis of diseases in which there is impaired movement of fluid. Studies in the AQP4-null mouse model have provided evidence that AQP4 serves as an influx route for water in conditions associated with congenital obstructive hydrocephalus[12]. In a mouse model of ischemia, AQP4-null mice have a thicker inner retina and more cells than the wild-type mice[13]. In the CNS, studies have shown that water flux through perivascular AQP4 is essential for removing K^+ after neuronal activation and mislocalized AQP4 may lead to delayed K^+ clearance[14]. Therefore it is not surprising that decreased seizure thresholds were found in AQP4 deficient mice[15].

Glaucoma leads to visual loss, and elevated intraocular pressure (IOP) is a major risk factor. AQP4, with its highly effective water transport function, may be involved in the pathological process of glaucomatous neuropathy. In rat, Yang et al[16] observed increased AQP4, and AQP9 (found in ganglion cells) expression in the region of the optic nerve of rats with experimentally elevated IOP. In two rat experimental glaucoma models, Dibas et al[3] observed decreased retinal AQP4 mRNA and protein levels, but increased expression of the intermediate fiber protein, GFAP, whereas in optic nerve astrocytes, there was enhanced expression of AQP4, which was co-localized with enhanced GFAP expression. The authors suggested that the hypertrophy of optic nerve astrocytes may be due to the increase in expression of AQP4 in rats with experimental glaucoma[3]. However, one study in postmortem human glaucoma eyes reported no alteration from normal eyes in retinal AQP4, but the retinal distribution of the aquaporin was not described[17]. Remodeling of astrocytes in the optic nerve head of human eyes with glaucoma and nonhuman primate (NHP) eyes with experimental glaucoma can have significant effects

on the retinal ganglion cells and their axons[18], and AQP4 could be involved in the glial scaring[19].

Inward rectifying potassium channel: Kir4.1

There is a large family of Kir channels. The family contains seven subfamilies (from Kir1.x to Kir7.x) classified by different subunit genes. The family also can be divided into four different functional groups: constitutively active (Kir2.x); G protein-gated (Kir3.x); ATP-sensitive (Kir6.x) and potassium transport (Kir1.x 4.x 5.x and 7.x)[20]. (Figure 1-3)

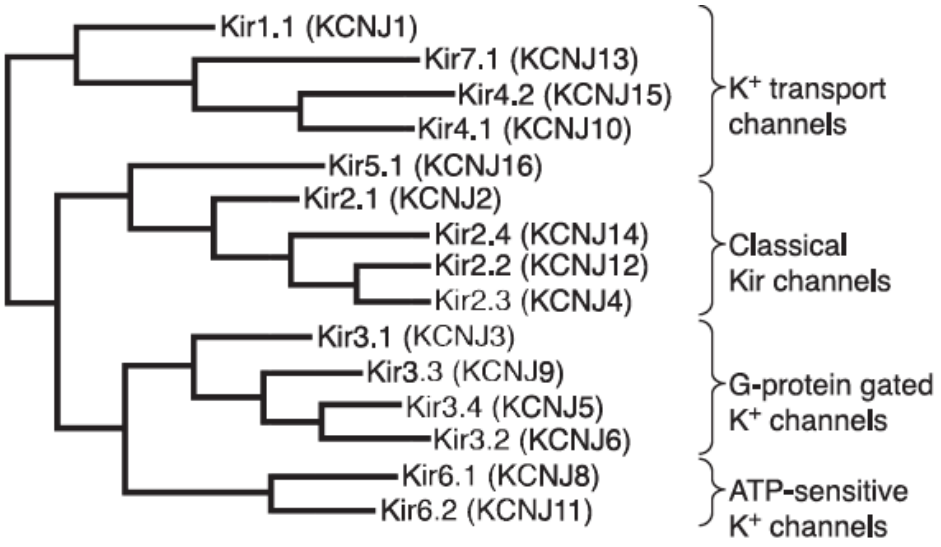

Figure 1-3 Basic structure and Kir channel phylogenetic tree[20].

When neurons depolarize, they release potassium ions (K^+) into the extracellular space, which increases the extracellular K^+ concentration $[K^+]_o$. In the retina, the K^+ ions in regions of high $[K^+]_o$ are taken up into Müller glial cells via their Kir4.1 channels, and redistributed to regions with lower $[K^+]_o$, e.g. the vitreous, the subretinal space and the vasculature of the neural retina[21]. This process, called "K^+ spatial buffering" or "K^+ siphoning" prevents K^+ accumulation in the extracellular space[22-24]. Removal of released K^+ is necessary because excessive $[K^+]_o$ will cause neuronal hyperexcitation and

neurotoxicity. The regional distribution in the Müller cells of inward rectifying K^+ channels (Kir4.1), which are essential for K^+ buffering, is appropriately polarized, with the highest levels of expression at glial-vascular and glial-vitreal interfaces[22, 24]. Kir4.1 immunoreactivity has been found in clusters in mammalian retina throughout the Müller cell membrane, and this clustering may be regulated by insulin and laminin signals[25].

The electroretinogram (ERG) is a clinical electrodiagnostic test that reflects the electrical activity of the different retinal components in recorded responses to short or long-duration flashes of light. Normally, the photopic a-wave reflects cone photoreceptor and Off cone bipolar cell activity, b-wave reflects the activity of On (and Off) cone bipolar cells, oscillatory potentials are thought to reflect the activity of amacrine cells. In patients with open-angle glaucoma (OAG) or ocular hypertension and monkeys with experimental glaucoma, a negative potential after the b-wave in the photopic ERG, called the photopic negative response (PhNR), is reduced in amplitude[26, 27]. The PhNR also has been found to be reduced in amplitude following intraocular injection of drugs known to suppress action potentials of retinal ganglion cells (RGCs)[26]. These findings provide evidence that PhNR in primate and other mammalian photopic ERG reflect the inner retina, specifically RGCs. In the scotopic ERG, there is a negative-going scotopic threshold response (STR) that also arises from inner retinal ganglion cells, or amacrine cells. The STR has been shown to be mediated by currents generated when Müller glia move the K^+ released from depolarizing inner retinal neurons into the ECS from regions of high K^+ concentration to regions of lower concentration[28]. Recent reports indicate that PhNR is generated not only by spiking inner retinal neurons, but also is mediated by K^+ currents in glial cells. Damage to glial cells, especially to ion and water balance, could decrease the amplitude

of PhNR. Accordingly, patients with Kir4.1 mutations and EAST syndrome (epilepsy, ataxia, sensorineural deafness and a renal tubulopathy)[29] have been observed to have reduced PhNR amplitudes. Taken together, these findings raise the possibility of change in Kir4.1 function in glaucoma.

The Kir4.1 subtype is a key channel in K^+ transporting glia in the CNS, and has been observed in astrocytes, oligodendrocytes, cerebellar Bergmann glia, and retinal Müller glia. Kir4.1 channels are weakly rectifying as homomeric channels, and strongly rectifying when heteromeric with Kir2.1 or Kir5.1[30]. In a rat chronic ocular hypertension model, Yang et al[31] observed down-regulated Müller cell Kir4.1 expression and attenuation of the peak inward potassium current. In a rat ischemia model, reduced Kir4.1 channel expression in Müller glia also has been described and associated with low amplitude STR[32]. In ocular tissue, K^+ spatial buffering and volume changes are spatially and temporally coupled, and both AQP4 and Kir4.1 are involved in K^+ spatial buffering and water flux. Expression of the two channels can be simultaneously altered in pathological changes in neural tissue. For example, there was an alteration in the location of Kir4.1 and AQP4 proteins in Müller glial cells due to excessive light exposure in rats[33], which caused edema in the outer retina. A recent study also shows abnormal expression of AQP4 and Kir4.1 in the brainstem and cortex of a rat model of amyotrophic lateral sclerosis[34], expression of Kir4.1 decreased, and expression of AQP4 increased[34], which supports the idea that K^+ buffering and volume changes are spatially and temporally coupled. The present study focused on the expression of AQP4 and Kir4.1 in the retina of a nonhuman primate model of experimental glaucoma. We were interested in

the status of these channels in the retinal nerve fiber layer (RNFL) near the optic nerve head.

RNFL near the optic nerve head

In retina near the optic nerve head in monkey, the RNFL is much thicker than in other regions, because retinal ganglion axons from the entire retina gather together to enter the optic nerve head (Figure 1-4 Left). Vertical sections of retina near the optic nerve head are made up of retinal ganglion cell axons, Müller cell trunks and astrocytes (Figure 1-4 Right) The density of Müller glial cells near the optic nerve head decreases relative to the foveal region of retina, whereas the density of astrocytes increases[35, 36]. Astrocytes near and within the optic nerve head have flattened cell bodies and a fibrous series of radiating processes[37]. The processes become elongated near the nerve, dividing the axons of retinal ganglion cells converging on the nerve into nerve fiber bundles. As the main glial cell in the nerve, astrocytes have many functions, similar to those of Müller glial cells, including regulation of ionic homeostasis, and as not yet mentioned in this proposal, synchronization of neuronal firing, neurotransmitter uptake, and glucose metabolism[38]. Glaucoma may alter glial function in the retina and optic nerve head.

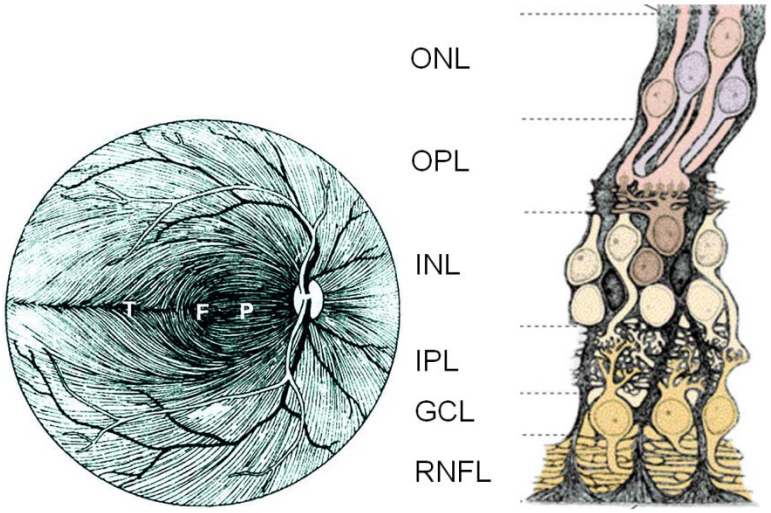

Figure 1- 4 The axon course map based on Shields[39] and a diagram that depicts retinal layers and location of retinal glia. (http://intranet.tdmu.edu.ua/)

Using immunohistochemistry, the present study will focus on the distribution of AQP4 and Kir4.1 in macaque monkey retina which is very similar to that of humans. Although the distribution of the Kir4.1 and AQP4 channels are well described in rodent retina[10], there is less specific information about these two channels in primate retina and the roles that they might play in ionic and osmotic homeostasis. Because we are interested in the effects of experimental glaucoma on the distribution of the channels, we will investigate regions in the monkey retina near the optic nerve head where clinical optical coherence tomography (OCT) tests are commonly used to measure the thickness of the retinal nerve fiber layer and to monitor the severity of the neuropathology. In those regions, nerve fiber bundles have formed and both Müller cells and astrocytes are normally present. We will compare normal monkey eyes and fellow eyes with experimental glaucoma. Altered immunolabeling and cellular distribution of Kir4.1 and AQP4 in eyes with experimental glaucoma will suggest abnormal glial cell activity, and may provide new insights on the pathophysiology of glaucoma.

Research questions addressed in this thesis

As noted above, the location of AQP4 and Kir4.1 in glial cells of the rodent retina, particularly in the Müller cells has been described previously. In rats and mice the two channels are co-localized, and they are concentrated in the endfeet that face the vitreous body, the subretinal space and the inner retinal vasculature. The present study will describe the immunolabeling of the two channels in the macaque monkey retina. The distribution of AQP4 and Kir4.1 may provide insights about ionic and osmotic homeostasis in monkey retina, and how they are affected by experimental glaucoma. This will be investigated in Specific Aim 1.

<u>Specific Aim 1:</u> To determine the distribution of AQP4 and Kir4.1 in Müller glia cells and astrocytes in the peripapillary region of the normal retina of macaque monkey.

a. To investigate the location of AQP4 and Kir4.1 in the retina of Rhesus monkeys using immunohischemistry

b. To determine whether AQP4 and Kir4.1 co-localize, as has been observed in rodent retinas.

AQP4 and Kir4.1 have both been observed to change their distributions in rodent models of experimental glaucoma[17, 31]. Expression of AQP4 was found to be reduced in Müller cells and increased in optic nerve astrocytes, along with GFAP[3]. Examination of the peripapillary region of the monkey retina in the present study provides an opportunity to examine effects of experimental glaucoma on Müller cells and the astrocytes associated with axon bundles in the retinal nerve fiber layer. It is hypothesized that there will be changes in the distribution of both types of channels, because AQP4 and Kir4.1 are co-

localized in rodents, they are both involved in spatial K^+ buffering and water flux, and they were affected by experimental glaucoma in monkeys. This will be investigated in Specific Aim 2.

<u>Specific Aim 2</u>: To investigate changes in distribution of AQP4 and Kir4.1 in eyes with experimental glaucoma.

a. To compare the location of AQP4 and Kir4.1 in the control eye with the location in the experimental glaucoma eye.

b. To determine whether the distribution of AQP4 and Kir4.1 differs by retinal region in control and experimental glaucoma eyes.

Chapter 2

Aquaporin 4 in retinal glial cells of normal macaque monkey eyes and eyes with experimental glaucoma

Introduction

Glaucoma is a heterogeneous group of potentially blinding diseases that cause damage to the optic nerve and the retinal ganglion cells whose axons form the nerve. There is increasing evidence that retinal and optic nerve head (ONH) glial cells are altered in glaucoma and are involved in the pathogenesis of disease. An important role of glial cells in the normal retina and central nervous system (CNS) is maintenance of the ionic and osmotic balance in the tissue. For osmotic balance in retina and CNS, the most prominent glial water channel is Aquaporin 4 (AQP4).

AQP4 belongs to a family of 13 known aquaporins[1]. Aquaporins facilitate water transport across membranes when there are differences in osmotic or hydrostatic pressure inside and outside of cells. In the rodent retina, AQP4 is mainly expressed in the endfeet membrane domains of Müller glial cells, where it is largely co-localized with Kir4.1 channels[11]. Spatial co-localization of AQP4 and Kir4.1 proteins in Müller glial cell endfeet regions facing the vitreous and blood vessels of the mammalian retina suggests that they are both involved in rapid water and potassium fluxes[11] and that K^+ buffering and tissue volume changes are spatially and temporally coupled[40].

In human eyes, and those of NHPs, the peripapillary region of the retina contains both Müller cells and astrocytes associated with axon bundles in the retinal nerve fiber layer (RNFL). Therefore, the peripapillary region provides an opportunity to examine effects of experimental glaucoma in a NHP model on Müller cells and astrocytes in the same tissue.

In this chapter, we will focus on the distribution of AQP4 in macaque monkey whose retina is very similar to that of humans. We will investigate regions near to the ONH where optical coherence tomography (OCT) is used clinically to measure the thickness of the retinal nerve fiber layer. In this region, nerve fiber bundles that will enter the optic nerve head are surrounded by trunks of Müller cells. We will compare normal monkey eyes with eyes with experimental glaucoma. Altered immunolabeling and cellular distribution of AQP4 in eyes with experimental glaucoma will suggest abnormal glial cell activity.

Methods

Animals

Five Rhesus macaque monkeys ranging in age from 7 to 11 years of age were subjects for this study. These animals were used in other studies as well[41]. Unilateral experimental glaucoma was created in five monkeys: OHT-57, OHT-60, OHT-61, OHT-64 and OHT-66. Experimental glaucoma was created in one eye by Argon laser scarification of the drainage angle to restrict the outflow of aqueous humor from the anterior chamber, the fellow eye served as a control[42]. Several laser treatments were necessary to create sustained elevation of IOP and to initiate optic neuropathy. The effects of experimental glaucoma were assessed over periods of 2 to 14 months after elevation of IOP[43]. During experimental glaucoma, perimetry, optical coherence tomography (OCT) and electroretinogram (ERG) testing was done for both the experimental (lasered) and fellow control eyes. Animals in the later stages of experimental glaucoma developed significant visual field defects, RNFL loss, and reduction of ganglion cell related ERG components. Table 1 shows which eye was laser-treated, the thickness of RNFL from the last OCT

scan before the monkey was sacrificed, and the regions around the ONH that were sectioned and analyzed in the confocal images. All experimental and animal care procedures adhered to the ARVO statement for the Use of Animals in Ophthalmic and Vision Research, and were approved by the Institutional Animal Care and Use Committee of the University of Houston.

Table 2-1 Subject Information

Animal	Experimental **Eye**	**Average RNFL thickness from final scan (μm)**			**Analyzed Regions****
		Con	Exp	% loss of RNFL*	
OHT-57j	Left	112.2	93.6	17%	I, S
OHT-60n	Left	102.4	61.8	40%	I, S
OHT-61o	Right	112.8	59.3	47%	I, N
OHT-64A	Right	103	74	28%	I, N, S
OHT-66s	Right	98	46	53%	I, N, S

*: 100 x (Con-Exp/Con)

**Within 5 mm of the optic nerve head

After final functional and structural assessments, the monkeys were deeply anesthetized and their eyes, with the optic nerve attached, were enucleated. The anterior segments of the eye were separated from the globe and the posterior segments of the eyes were fixed in 4% paraformaldehyde in 0.1M phosphate buffer. After one hour, the eyes were stored in a fresh solution of 4% paraformaldehyde at 4°C[44].

Immunohistochemistry

Immunofluorescence was used to detect Aquaporin 4 and glial markers in the retina. Tissue samples from the monkey retinas, approximately 5 mm in length, were taken within 5 mm of ONH, in the vicinity of the OCT peripapillary scan, and from three different areas: nasal, interior and superior regions of retina, where the RNFL dominated the retina (Table. 1). Samples were embedded in ultra-low gelling temperature agarose (Sigma-Aldrich A3038-10G), and cooled to 4°C for 30 mins to 1 hour. Vibratome sections of retina were cut at a thickness of 40 μm (Leica VT 1000S) and stored at 4°C in phosphate buffer. Before antibody treatment, retinal sections were incubated for 10 min in 10 mM sodium citrate (pH 6), at 86 °C in a water bath for antigen retrieval. These samples were cooled to room temperature, then washed with PBS and non-specific antibody binding was blocked in 5% normal donkey serum contain 0.3% Triton X-100, and 0.1% sodium azide in PBS for three hours on a shaker at 4°C. The sections were exposed to mouse anti-aquaporin-4 antibody (1:250), rabbit monoclonal glutamine synthetase (GS) antibody (1: 125) and goat anti glial fibrillary acidic protein (GFAP) antibody (1:250) diluted in PBS containing 1% normal donkey serum, 0.3% Triton X-100, and 0.1% sodium azide overnight on a shaker at 4°C (Table. 2). To show the neural components of the RNFL, some sections were exposed to rabbit anti-neurofilament light chain antibody (NF; 1:500), mouse monoclonal GS antibody (1:250), and goat anti-GFAP antibody (1:250). All sections were washed in PBS 6*30 minutes, and then incubated with a mouse conjugate of fluorescein (1:250), Cy3-conjugated donkey anti-rabbit IgG (1:250) and Cy-5 conjugated donkey anti-goat IgG (1:250) for 3 hours

followed by PBS washes 5*30 minutes[3]. In the end, sections were put on to slides and mounted with fluorescence mounting medium (Vector Vectashield H-1000)[44].

Table 2-2 Antibody List

Antigen	Host	Dilution	Source	Reference
Aquaporin 4 [3D2]	Mouse	1:500-1:1000	AbCam, Cambridge, MA (Ab11026)	Parfenova H et al., 2012
Glial fibrillary acidic protein (GFAP)	Goat	1:250	AbCam, Cambridge, MA (Ab53554)	Bettum IJ et al., 2014
Glutamine Synthetase (GS)	Rabbit	1:125	Sigma-Aldrich, St. Louis, MO (G2781)	Alexandre S Basso et. al, 2008
Neurofilament Light Chain	Rabbit	1:250	Thermo Fisher, Rockford, IL (PA5-34650)	
Cy™5 AffiniPure IgG (H+L)	Donkey anti-Goat IgG	1:250	Jackson ImmunoResearch (Code: 705-175-147)	--
Cy™3 AffiniPure F (ab')$_2$ Fragment IgG (H+L)	Donkey anti-Rabbit IgG	1:250	Jackson ImmunoResearch (Code: 711-166-152)	--
Donkey Anti-Mouse IgG H&L (Alexa Fluor® 488)	Mouse	1:250	AbCam, Cambridge, MA (ab150105)	Poulsen JN et al., 2014

Imaging

Images of retina were taken from control and experimental glaucoma eyes using identical parameters with a laser-scanning confocal microscope (Leica, Confocal system TCS SP2; 20 x and 63x lens; 1024*1024 format). Stacks of serial optical sections, 0.5µm thick, were collected from the sections for the three different laser wavelengths, and different pseudocolors generated to identify and localize the antibodies: red for GS, blue for GFAP, green for AQP4 and white for NF. The images of control and experimental eyes

were examined further using Image J software or Photoshop Cs2 (Adobe Systems, Inc., Mountain View, CA) and pseudocolored images were merged to identify regions of co-localization.

Results

Immunolabeling of AQP4 and glial markers in macaque monkey control eye

Previous studies determined the expression pattern of AQP4 in the rat retina, which mainly was located in the inner retina and outer plexiform layer[45]. Herein, we investigated the distribution of AQP4 in the macaque monkey model of unilateral experimental glaucoma. We first looked at AQP4 labeling in control eyes. In our experiments, only one eye of each monkey was laser-treated, the other eye served as the control and was assumed to be a normal eye.

Figure 2-1 shows images from the control eye of experimental glaucoma monkey OHT-60. Figure 2-1 A shows immunolabeling for GS (red) which is known to be in Müller cells. The labeling is strong in the OPL, it is lighter in the INL where the somas are located, and it is strong in the Müller cells trunks that surround the nerve bundles. Figure 2-1B shows labelling for GFAP (blue) mainly in astrocytes in the RNFL region (Figure 2-1 B). In the merged image (Figure 2-1 C), the red and blue colors remained separate indicating that GS and GFAP were not co-localized. Therefore, GS and GFAP can be used to distinguish the Müller cells and astrocytes in the control eye. Figure 2-1 D, shows labeling for AQP4 (green). It was located prominently in regions similar to those labelled for GS, i.e. the Müller cells. As in the Müller cells, AQP4 labeling was strong in the outer plexiform layer (OPL), and in processes surrounding the nerve fiber bundles in

the inner retina. In addition it was in some processes surrounding blood vessels, and unlike the labeling for GS, light staining was found in the region of the nerve fiber bundles. Figure 2-1, E and F show immunolabeling for neurofilament, confirming that the normal RNFL is largely composed of axons from retinal ganglion cells (white), compared to the glial components (red and blue).

Figure 2-1 near here

Double labeling of AQP4 and glial marker in control eyes

To confirm the generality of the location of GS and GFAP, and distribution of AQP4 seen in OHT-60, three additional control monkeys retinas were immunolabeled for AQP4 and GS (OHT-57, OHT-61 and OHT-66; Figure 2-2). A similar distribution of AQP4 labeling was seen in these control eyes as was seen in OHT-60 (Figure 2-2 first row). The second row in the figure shows labeling for GS in the same sections. In the merged images in the third row, co-localization of the markers for AQP4 and GS is obvious in regions that are orange or yellow, due to overlapping of red (GS) and green (AQP4) staining. This co-localization confirms the presence of AQP4 in Müller cells in the control eyes, although the labeling was somewhat variable in the different animals. The results are seen best in the sections from OHT-66 that are shown at twice the magnification of the other sections. A group of processes in the nerve fiber bundles were AQP4 positive in all animals, i.e. green staining in that region, but did not become orange or yellow in the merged images. This staining for AQP4 may have been in astrocyte processes.

Figure 2-2 near here

To determine if AQP4 was in the astrocytes, in Figure 2-3, we merged the same images that are shown in Fig. 2.2 top row, immunolabeled for AQP4 (green) with images stained for GFAP (blue) shown in Figure 2-3 middle row. GFAP was located in the RNFL, within the nerve bundles, as described for Figure 2-1. The merged images (Figure 2-3 third row), show that the majority of the GFAP positive processes changed from bright blue to a lighter more aqua color, indicating that the astrocytes were weakly positive for AQP4. Taken together, these finding indicate that in the control eye of the experimental glaucoma monkey, AQP4 was strongly expressed in the Müller cells and more weakly expressed in the astrocytes.

Figure 2-3 near here

We also labeled additional locations within 5 mm of the ONH to see if the AQP4 distribution was similar across regions. A comparison of the images from inferior (Figure 2-4 A, B, C), superior (Figure 2-4 C, D, E), and nasal (Figure 2-4 F, G, H) regions for OHT-66, shows that for all regions AQP4 labeling was strongest in the Müller cells with light labeling in astrocytes. These findings were confirmed in three additional monkeys (see appendix, Fig. A-1). We concluded that AQP4 in control retina was predominately located in the Müller cells, regardless of the region near the ONH.

Figure 2-4 near here

Immunolocalization of AQP4 and glial marker in macaque monkey control eye and experimental eye

To determine whether experimental glaucoma affected AQP4 expression, we did the same immunolabeling experiments on experimental eyes that was done in control eyes

and compared the labeling in the two eyes. Retinas of four monkeys, OHT-57, OHT-60, OHT-61 and OHT-66 stained for AQP4, are shown in Figure 2-5, with control eyes on the left, and experimental eyes on the right. In this figure, the animals are arranged from top to bottom, in the order of relative RNFL loss, determined from SD-OCT scans of the RNFL thickness. The retinal sections of control and experimental eyes are aligned at the level of the OPL. The figure shows that the retinas all became thinner in the region of the RNFL. Retinal ganglion cell loss was most obvious for OHT-61 and 66, and in OHT-66, the most severely affected animal, the IPL also was thinner in the experimental eye than in the control eye. AQP4 in the experimental eyes show an altered pattern of immunolabeling compared to that found in the control eyes Retinas of eyes with experimental glaucoma showed a reduction of AQP4 labeling in the Müller cells, but increased labeling in the RNFL which was most obvious in OHT-66.

Figure 2-5 near here

In order to investigate how AQP4 expression and distribution in Müller cells vs astrocytes was affected by experimental glaucoma, double labeling for AQP4 and GS (for Müller cells) vs AQP4 and GFAP (for astrocytes) was examined in the same four monkeys' inferior regions that were shown in Figure 2-5. The double labeling for AQP4 and GS is shown in Figure 2-6. In the control eyes (left columns), the color in the merged images was orange to yellow showing that AQP4 was co-localized with GS in the Müller cells as described above. In contrast, in the experimental eyes (right column), the co-localization of AQP4 and GS was reduced. For OHT-57 (A, B) who had mild neuropathy with only 17% RNFL loss, there still was some co-localization of GS and AQP4 in the experimental eye, but both GS and AQP4 labeling appeared to be reduced.

Decreases in GS immunolabeling were reported in canine primary glaucoma in mildly damaged regions[46]. In monkey OHT-60 (C, D) with more severe damage, (40% loss of the RNFL in the experimental eye), yellow areas were less prominent in the experimental than the control eye. In OHT-66 (G, H; most affected with 53% loss of RFNL) double labeling in the control eye was yellow throughout the retina and in the Müller cell trunks, but in the experimental eye it changed to orange (less green, more red), indicating a reduction of AQP4 in Müller cells.

Figure 2-6 near here

Double labeling for AQP4 and GFAP is shown in Figure 2-7. The green and blue labeling varied in degree of overlap in the control eyes (left column), indicating varied content of AQP4 in astrocytes in these eyes. However, in the experimental glaucoma eyes, in the area where nerve bundles had been, the RNFL labeling was more bluish green (aqua) than it was in the control eyes. In OHT-57 (A, B), with mild neuropathy, the overlap of AQP4 and GFAP immunolabeling was just noticeable. In OHT-60 (C, D) the co-localization of AQP4 and GFAP was more obvious, and as described above, the labeling for AQP4 was reduced in the Müller cells (Figure 2-7 C, D). This change in the location of AQP4 labeling also was seen in an animal with even more severe neuropathy, OHT-61 and this retina also showed signs of stress in the Müller cells (GFAP staining). In general the findings for animals with different stages of neuropathy suggests that eyes with later stage neuropathy show a greater shift in AQP4 from Müller cells to astrocytes than eyes in early stages.

Figure 2-7 near here

The high magnification images of the retina from monkey OHT-66 with severe RNFL loss (Figures 2-6 and 2-7 G, H) show the changes due to neuropathy in the experimental eye more clearly. The overlaid images with the Müller cell marker GS (red) and AQP4 marker (green) show co-localization of GS and AQP4 in the control eye (Figure 2-6 G), whereas co-localization was reduced in the experimental eye. In contrast, Figure 2-7 G, H shows that AQP4 labeling increased in the astrocytes of the experimental eye, indicated by the overlap of with staining for GFAP bluish green (aqua) color (Figure 2-7 H).

Distribution of AQP4 in different regions of retina

Figure 2-8 shows results for control vs experimental eye for OHT-66 in three different retinal regions near the ONH. Across the images from inferior (Figure 2-8 A, B), superior (Figure 2-8 C, D), and nasal regions (Figure 2-8 E, F), the changes in AQP4 immunolabeling in the experimental eye were similar. In each case, the RNFL in the experimental eye was reduced compared to the control eye, and the astrocytes appeared to aggregate in the nerve fiber layer between the Müller cells trunks. Labeling for AQP4 in three addition animals is shown in the Appendix for the superior (Figure A-1) and nasal (Figure A-2) regions. The findings were similar to those described for Figure 2-8. There was a slight tendency for less loss of labeling for AQP4 in the Müller cells of experimental eyes in the superior region. Despite the differences in the extent to which labeling occurred, increased labeling for AQP4 could be seen in the astrocytes in all three regions.

Figure 2-8 near here

Triple immunolabing in control and experimental eyes

Figure 2-9 shows results for OHT-60 that summarize the changes in AQP4 in experimental glaucoma that were described above. To emphasize the labeling, the figure illustrates stacks of 10 sections, whereas all other images in this thesis are from single sections. In these images, the change from yellow or yellow green color in the control eye to orange color in the Müller cells in the experimental eye in double labeled images for AQP4 and GS is evident in all layers of the retina. The change is particularly obvious in panels G and H where triple labeling for AQP4 and the glial markers is shown. The co-localization of AQP4 with aggregated astrocytes in the RNFL region in experimental eyes is well illustrated in these triple labeled images.

Figure 2-9 near here

Discussion

AQP4, a water transport channel, has a key role for maintaining water balance and homeostasis in the ocular tissue. Our study provides strong evidence that AQP4 is involved in the pathological processes in experimental glaucoma. First we detected the immunolabeling for AQP4 both in the control eye and the experimental glaucoma eye, the distribution of AQP4 in control eyes was similar to that of AQP4 in normal rodents, which mainly localized in endfeet processes and perivascular structures[3]. AQP4 labeling generally was weakly co-localized with the GFAP positive astrocytes of the nerve fiber layer in the control eyes. However, in experimental glaucoma eyes, with nerve fiber loss, AQP4 was greatly reduced in Müller cells, whereas strikingly strong labeling was detected in GFAP positive astrocytes. The AQP4 positive astrocyte processes aggregated in the region typically occupied by nerve fiber bundles and remained surrounded by

Müller cell processes. To confirm that this shift of AQP4 labeling could be detected all around the optic nerve head, different areas were stained. We found that all areas showed the change in AQP4. We also found that the more complete shift in distribution of AQP4 was in eyes with the greatest nerve fiber loss.

Some studies indicated that enhanced neuronal activity increased extracellular water, and that the excess water may move into glial cells[47]. The reduction of AQP4 in Müller cells of glaucoma eyes could have caused a major deficit in water flux, particularly in inner retina. The increase in AQP4 immunolabeling suggests increased expression of AQP4 in astrocytes of glaucoma eyes. This is a pathophysiological alteration that might reflect a compensation for the loss of AQP4 mediated water movement, or other changes in neighboring Müller cells, and degenerating nerve fibers.

The existence of reactive Müller cells (gliosis) has been documented in many ocular disorders, including glaucoma[38]. Müller cell gliosis is commonly characterized by the enhanced expression of GFAP in the inner retina. Our study only showed signs of reactivity (GFAP staining) in two of the animals. There also have been reports that astrocytes participate in tissue remodeling[18]. Astrocytes are reported to synthesize growth factors and other cellular mediators that may affect the retinal ganglion cells[18]. AQP4 as a water channel in astrocytes may also contribute to the healing process. Our study confirmed that experimental glaucoma can cause astrocytes in the RNFL to express more water channels. Our findings differ from findings by Mizokami et al, who did not detect any expression of AQP4 in the ONH[48], but did find reduced expression of AQP9 around optic nerve head in laser-induced experimental glaucoma in a primate and in human eyes with glaucoma[48]. AQP9 is located in retinal ganglion cells, and we should examine the

changes of this aquaporin in our model in future studies. The alterations of AQP expression in glaucoma was tested by Yang et al in a rat model of experimentally elevated IOP[16]. They found increased AQP4 expression and co-localization with AQP9 in the region of ONH in rats with the elevated IOP and the increased expression of AQP4 was related to increased elevation of IOP[16]. Our findings in monkey that AQP4 immunolabeling was enhanced in astrocytes in the RNFL in eyes with the greatest neuropathy are consistent with this observation in rats.

Early studies had suggested that K^+ spatial buffering and volume changes are spatially and temporally coupled. AQP4 has exceptionally high water permeability, which serves as the major water channel in the glial cells. The distribution patterns of AQP4 also are similar to that of Kir4.1. (This is addressed more in the discussion in the next chapter)

In summary, this chapter reports that in monkey retinal regions near the optic nerve head, Müller cells normally show AQP4 expression from the OPL to inner limiting membrane with the strongest expression in OPL, perivascular regions, the trunks and vitreal endfeet of the cells. Our findings can be interpreted to mean that experimental glaucoma causes a shift in AQP4 expression from Müller cells to astrocytes, perhaps in an attempt to improve survival of the neurons.

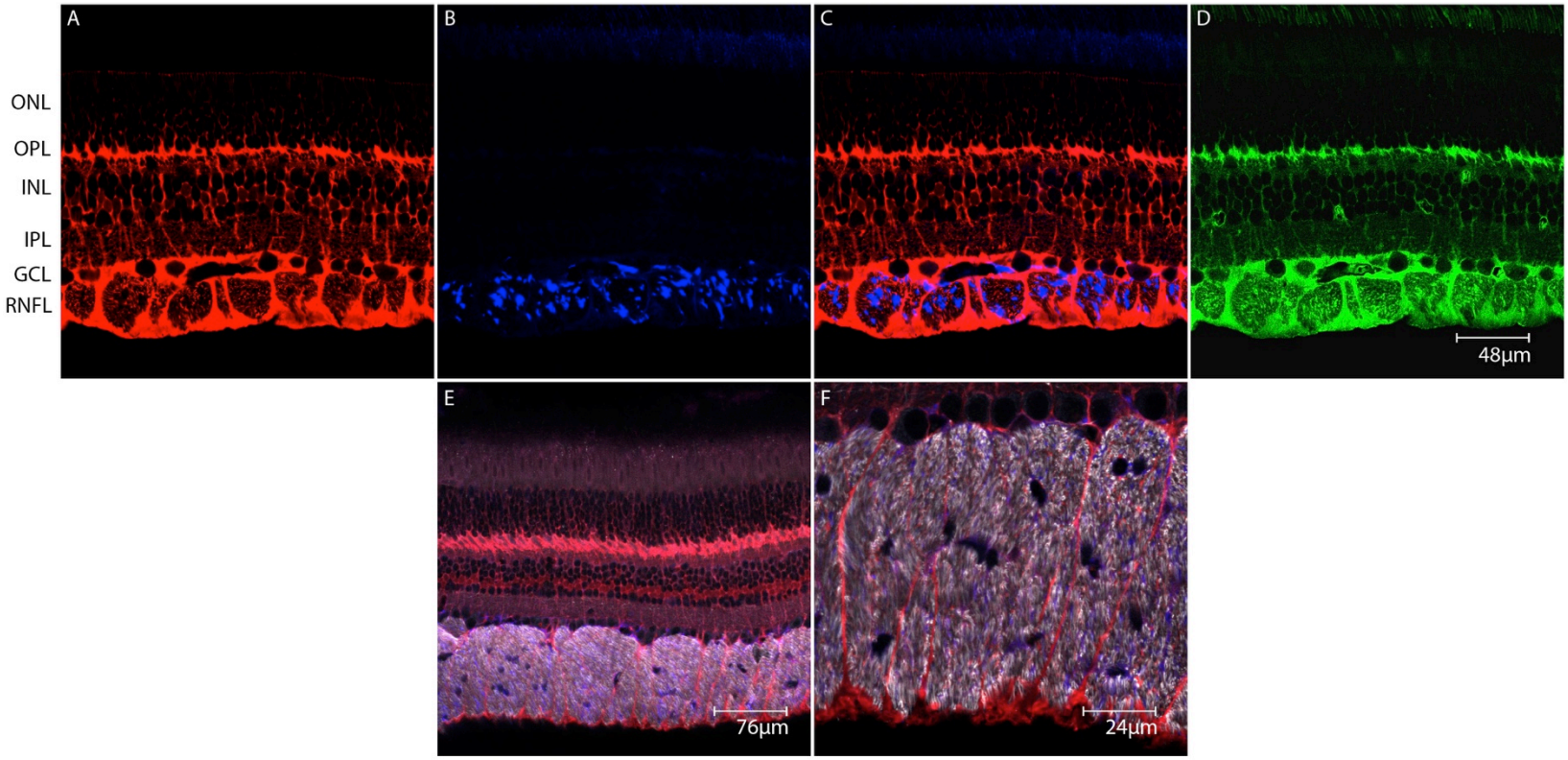

Figure 2-1 Immunolabeling for glial makers (GS, GFAP), and AQP4 in the retina of the control eye (OHT-60) and for neural filament marker along with s with the glial markers (OHT-66) within 5 mm of the ONH in the inferior region. **(**All images are 63x Zoom 1x, 1 section projection, 0.5µm) A. Labeling for the Müller cell marker, GS (red). B. Labeling for astrocyte marker, GFAP (blue). C. Merged images of GS and GFAP labeling. D. Labeling for AQP4 (green). E. Merged images of GS, GFAP and NF (white; 20x Zoom 2x, 1 section projection). F. High magnification of merged images, (GS, GFAP, NF: 63x Zoom 2x, 1 section projection).

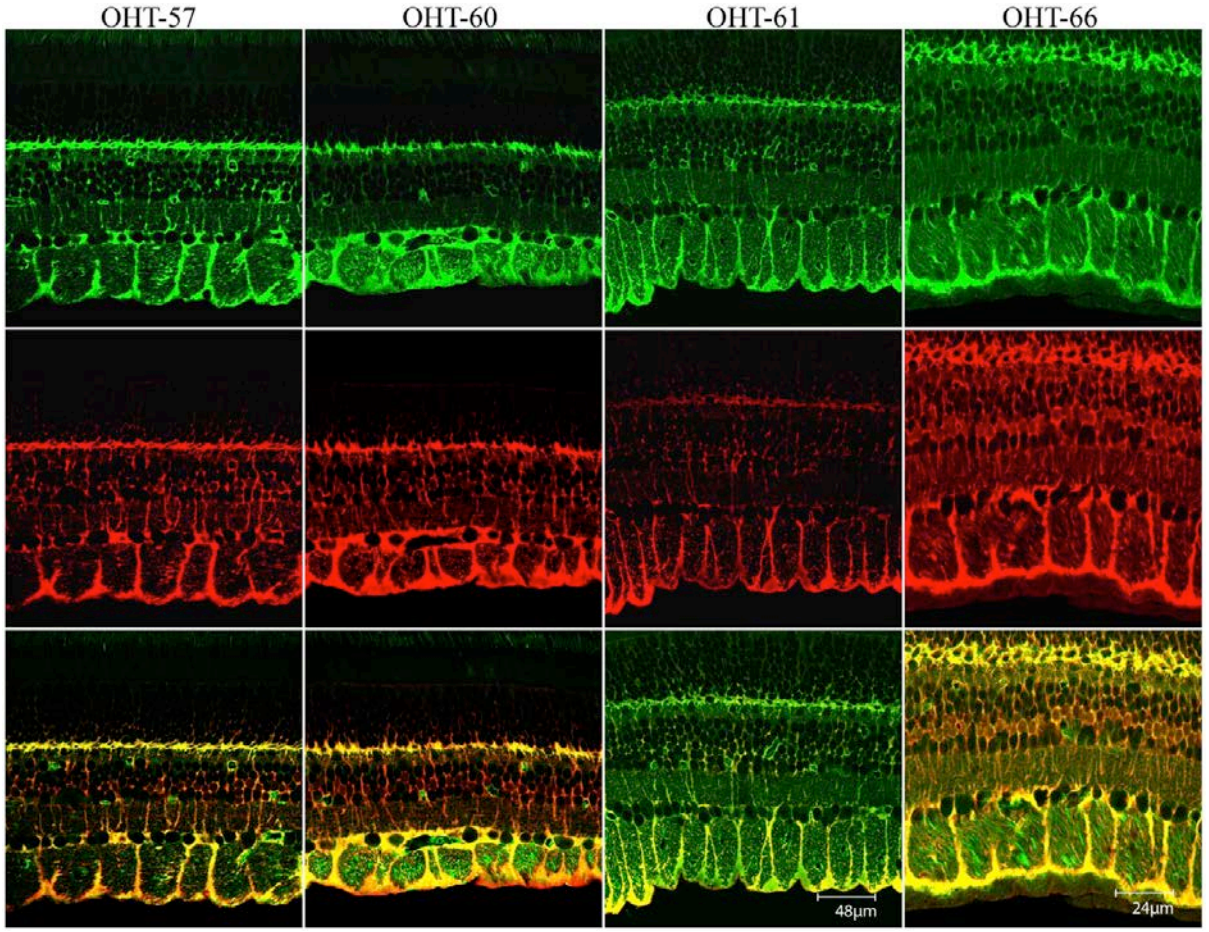

Figure 2-2 Double immunolabeling for AQP4 and the Müller cell marker, GS in the control retina within 5 mm of the ONH in the inferior region for four monkeys (OHT-57, OHT-60, OHT-61 and OHT-66). (Images for OHT-57, OHT-60 and OHT-61 are 63x Zoom 1x, 1 section projection, 0.5µm. Images for OHT-66 are 63x Zoom 2x, 1 section projection, 0.5µm). From left to right, the nerve fiber loss increased. The first row shows AQP4 labeling in all four normal monkey eyes. The second row shows the GS labeling and the third row shows the double labeling for AQP4 and the Müller cell marker GS.

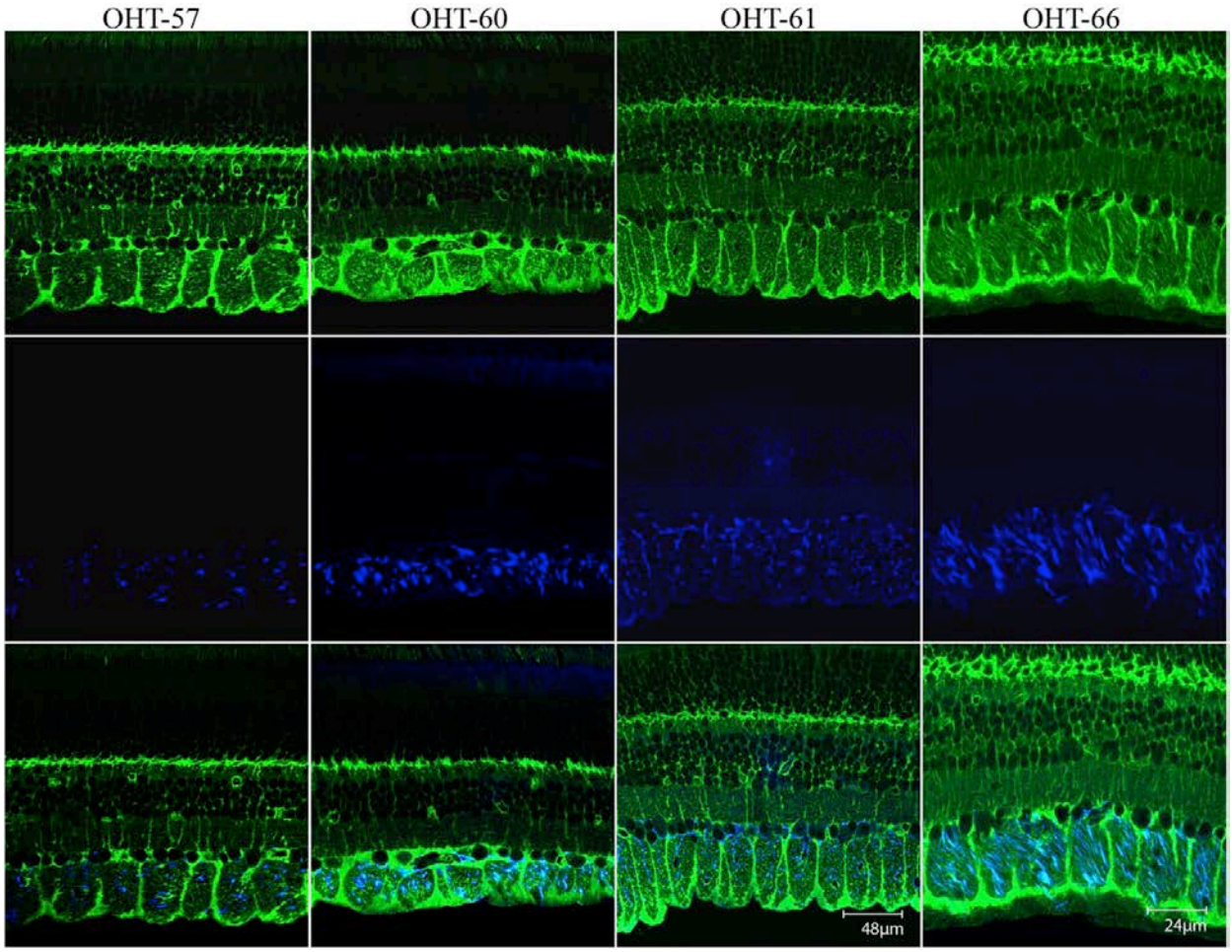

Figure 2-3 Double immunolabeling for AQP4 and glial maker GFAP in the retina of the control eye for four monkeys (OHT-57, OHT-60, OHT-61 and ONT-66) within 5 mm of the ONH in the inferior region. (Images for OHT-57, OHT-60 and OHT-61 are 63x Zoom 1x, 1 section projection, 0.5µm. Images for OHT-66 are 63x Zoom 2x, 1 section projection, 0.5µm). From left to right, the nerve fiber loss increased. The first row shows AQP4 in all four monkey eyes. The second row shows the GFAP labeling and the third row shows the double labeling for AQP4 and the astrocyte marker GFAP.

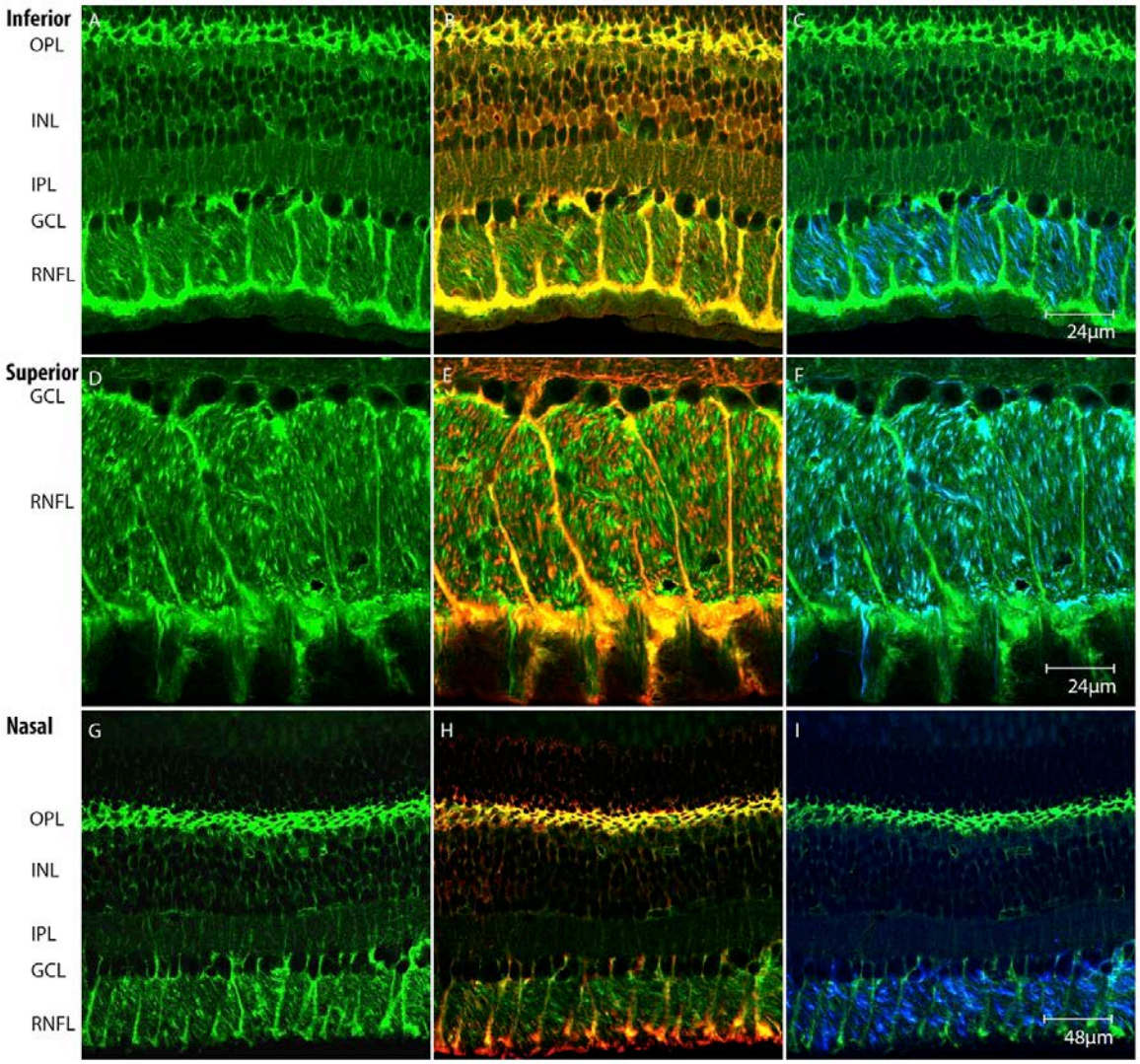

Figure 2-4 AQP4 and glial marker immunolabeling for the retina of the control eye of OHT-66 within 5 mm of the ONH in the inferior, superior and nasal region. (Images for A-F are 63x Zoom 2x, 1 section projection, 0.5µm. Images for G-I are 63x Zoom 1x, 1 section projection, 0.5µm). A-C: inferior region. D-F: superior region. G-I: nasal region. A, D, G: single labeling for AQP4. B, E, H: double labeling for AQP4 and GS. C, F, I: double labeling for AQP4 and GFAP.

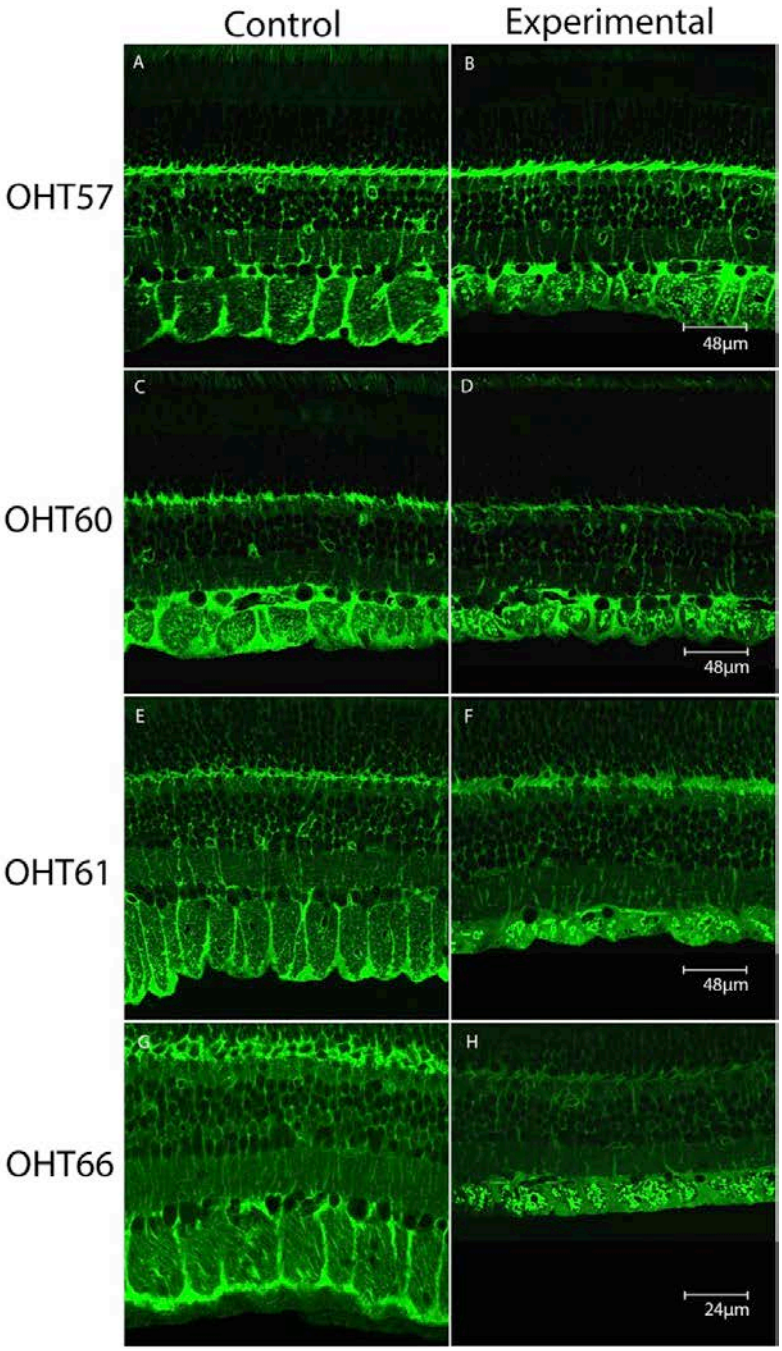

Figure 2-5 Labeling of AQP4 in the control and experimental retina within 5 mm of the ONH in the inferior region for four monkeys (OHT-57, OHT-60, OHT-61 and OHT-66). (Images for OHT-57, OHT-60 and OHT-61 are 63x Zoom 1x, 1 section projection, 0.5µm. Images for OHT-66 are 63x Zoom 2x, 1 section projection, 0.5µm) From top to bottom, the relative global nerve fiber loss increased in the experimental eye. The left column (A, C, E, G) shows the control eye, the right column (B, D, F, H) shows the fellow experimental glaucoma eye.

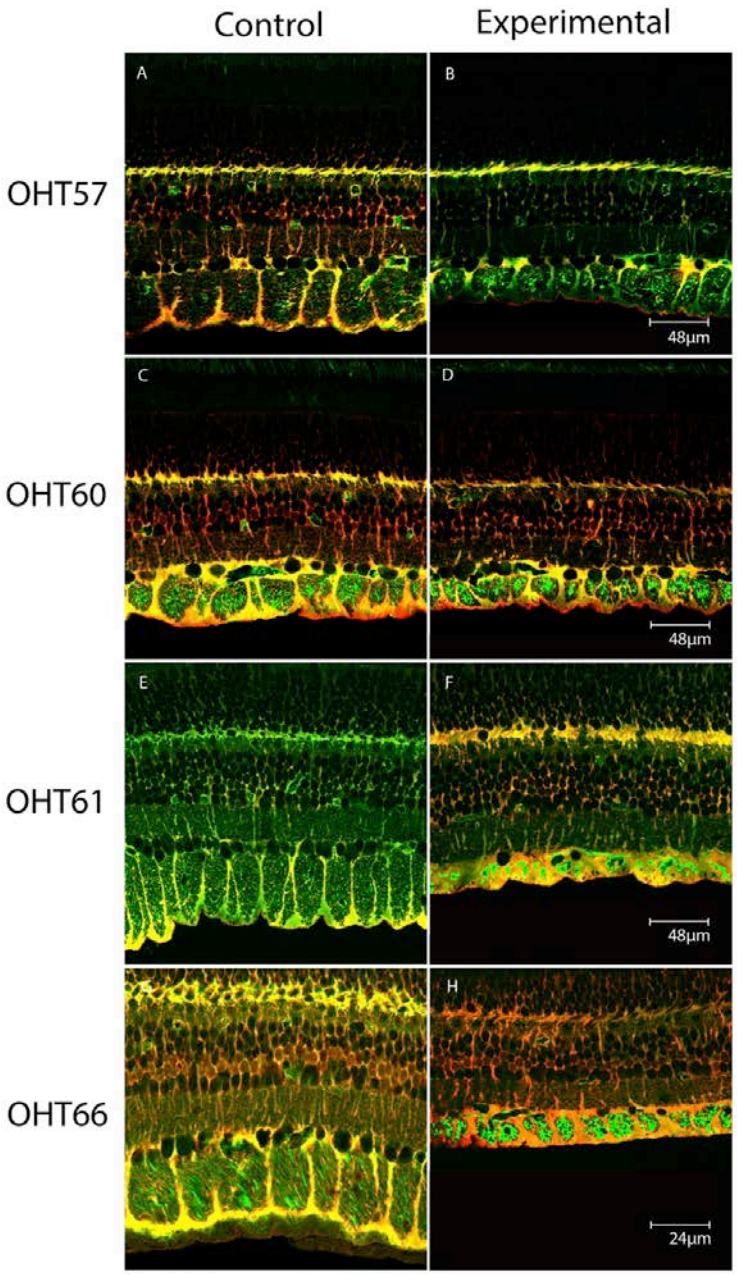

Figure 2-6 Double immunolabeling for AQP4 and GS in the control and experimental retina within 5 mm of the ONH in the inferior region for the same four monkeys whom AQP4 labeling was illustrated in Fig. 2-5. (Images for OHT-57, OHT-60 and OHT-61 are 63x Zoom 1x, 1 section projection, 0.5µm. Images for OHT-66 are 63x Zoom 2x, 1 section projection, 0.5µm). From top to bottom, the relative global nerve fiber loss increased in the experimental eye. The left column (A, C, E, G) shows the control eye, the right column (B, D, F, H) shows the fellow experimental glaucoma eye.

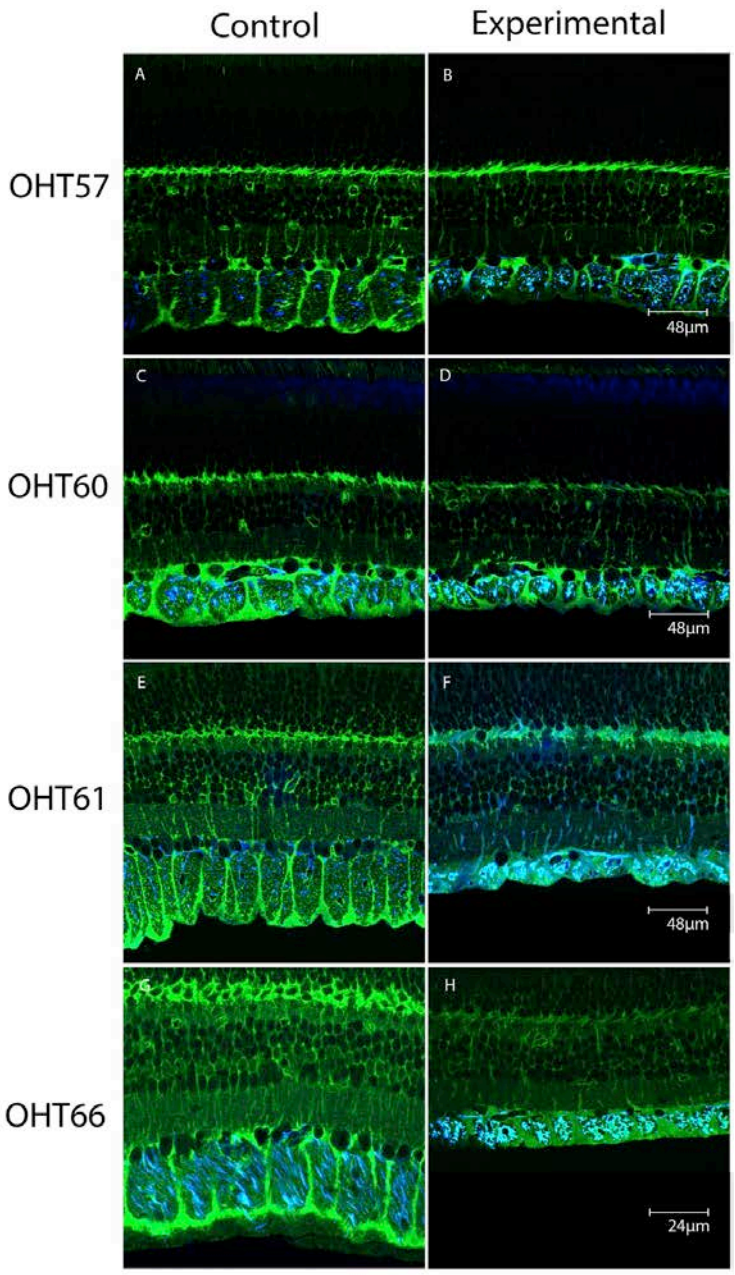

Figure 2-7 Double immunolabeling for AQP4 and GFAP for the control and experimental retina within 5 mm of the OHN head in the inferior region for the same four monkeys (OHT-57, OHT-60, OHT-61 and OHT-66) illustrated in Figures 2-5 and 2-6 above. (Images for OHT-57, OHT-60 and OHT-61 are 63x Zoom 1x, 1 section projection, 0.5µm. Images for OHT-66 are 63x Zoom 2x, 1 section projection, 0.5µm) The left column (A, C, E, G) shows the control eye, the right column (B, D, F, H) shows the experimental glaucoma eye.

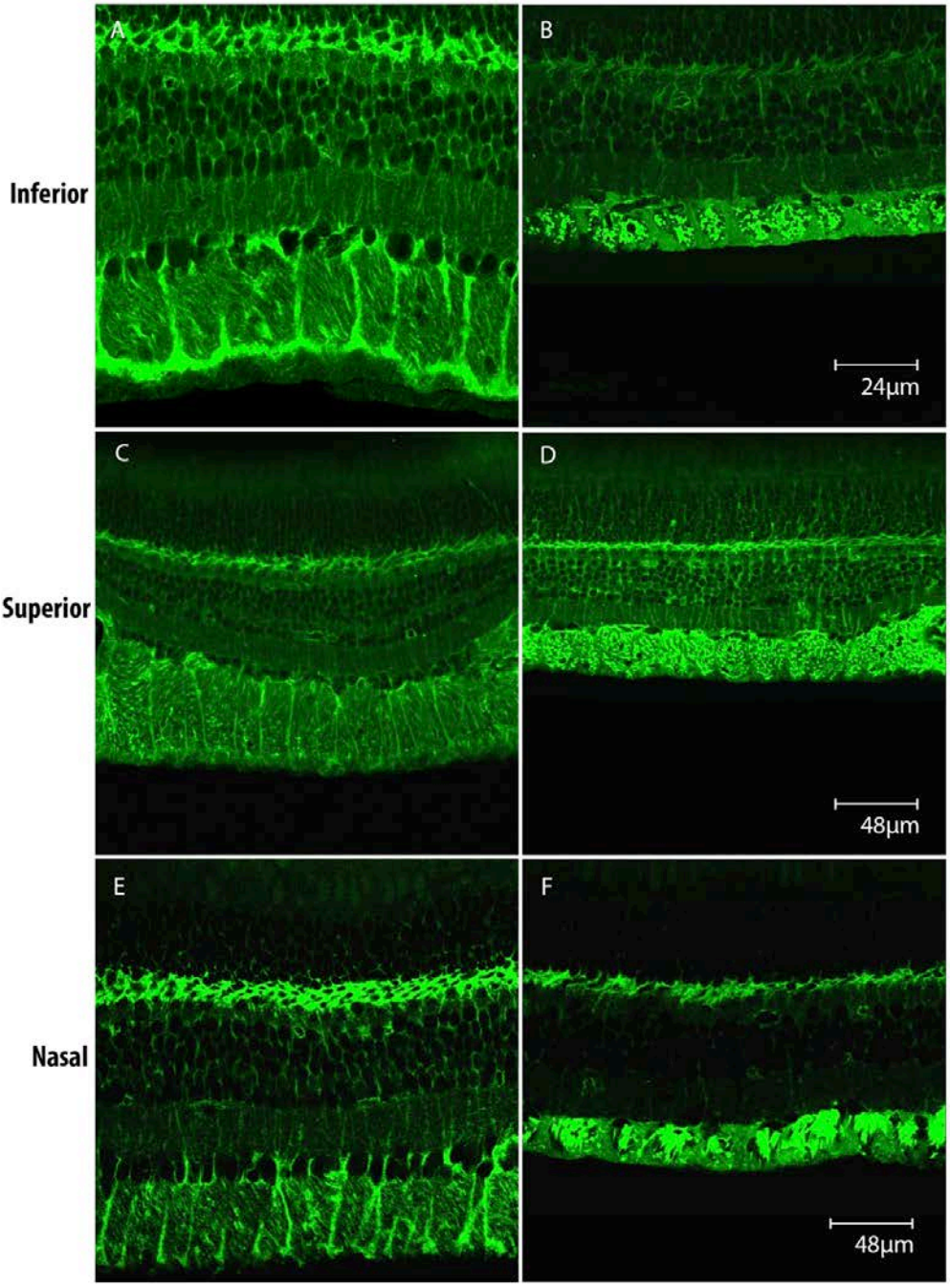

Figure 2-8 AQP4 immunolabeling for OHT-66 in inferior, superior and nasal regions of the retina within 5 mm of the ONH for the control eye and experimental eye. (Images for A-B are 63x Zoom 2x, 1 section projection, 0.5µm. Images for C-F are 63x Zoom 1x, 1 section projection, 0.5µm) A-B: inferior region. C-D: superior region. E-F: nasal region. A, C, E: control eye. B, D, F: experimental eye.

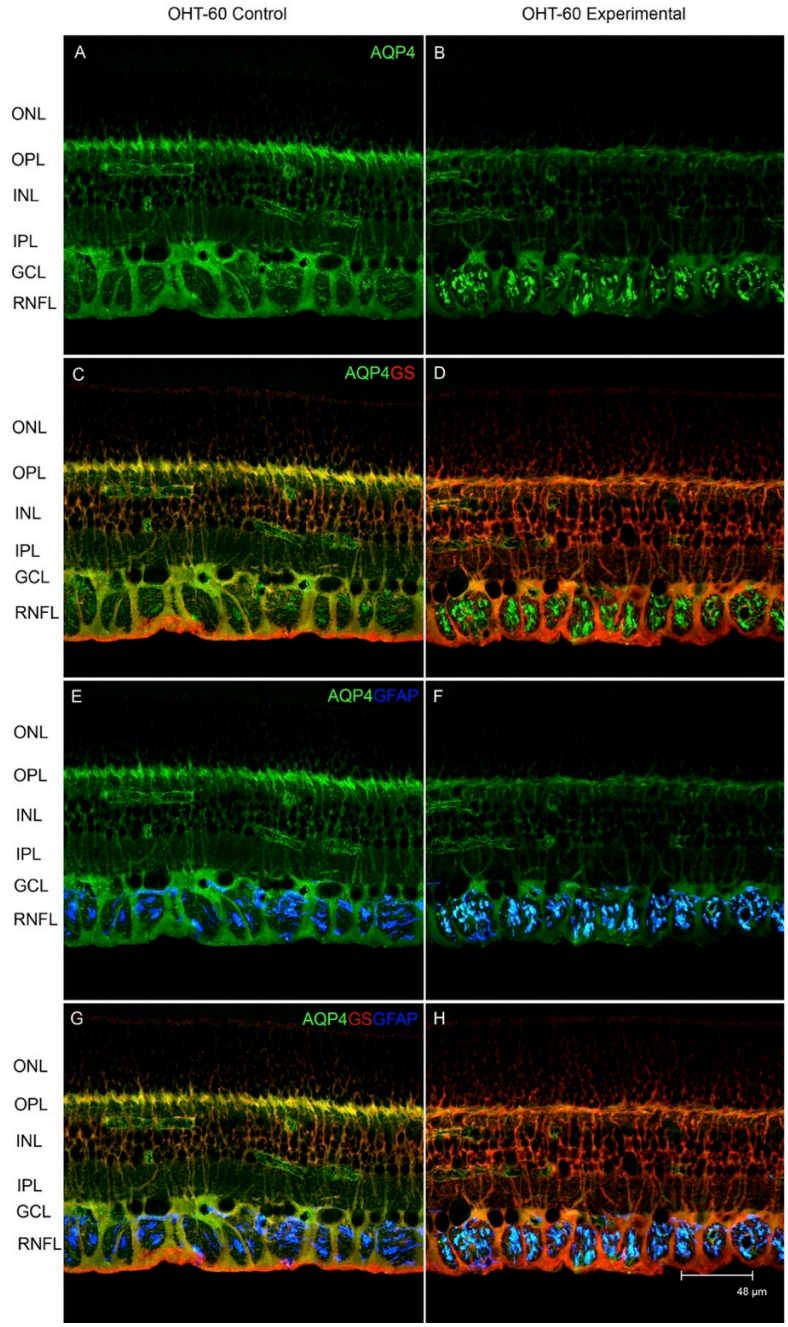

Figure 2-9 Immunolabeling for AQP4, GS, and GFAP in the control (Left) and experimental eye (right) for monkey OHT-60 (43% RNFL loss). Images A and B show AQP4; images C and D show AQP4 and GS; images E and F show AQP4 and GFAP, and images G and H show AQP4, GS, and GFAP. (Images are 63x Zoom 1x, 10 section projection, 0.5µm).

Chapter 3

Kir4.1 in retinal glial cells of normal macaque monkey eyes and eyes with experimental glaucoma

Introduction

Glial cells are important for maintaining ionic and osmotic balance in neural tissue. Müller glial cells as major macroglia in the retina, have an important role in removing the excess K^+ in the extracellular space of inner retina generated by depolarizing neurons The excess is moved to the subretinal space, blood vessels or vitreous. This process is called "spatial buffering". Inwardly rectifying potassium channels are transmembrane proteins that allow potassium ions to flow into cells more easily than out of cells, so that they generate a large potassium conductance that contributes to membrane potential and equilibrium potential of the cells in which they are located. Kir channels form a large family and have been found in a wide variety of cell types. They have been classified into seven subfamilies: Kir1.x to Kir7.x6. The K^+ spatial buffering through Müller cells is mediated predominantly via Kir4.1 channels[20]. Our study will focus on the Kir4.1 channels that are expressed in retinal macroglia and are potentially related to the experimental glaucoma.

Kir4.1 was initially found in the brain glial cells. It has been demonstrated that knock out of Kir4.1 is sufficient to remove K^+ permeability attributable to Kir channels in brain glia[49]. Kir4.1 was thought to be an essential component of Kir family and to be involved in the "K^+ buffering", which was important in mediating normal neuronal function. Later, Kir4.1 was detected in the retinal Müller cells, with Kir4.1 homomeric in the endfeet facing the vitreous and blood vessels, and in some studies, with Kir41 heteromeric with Kir5.1 in the perisynaptic processes[50] (Figure 3-1).

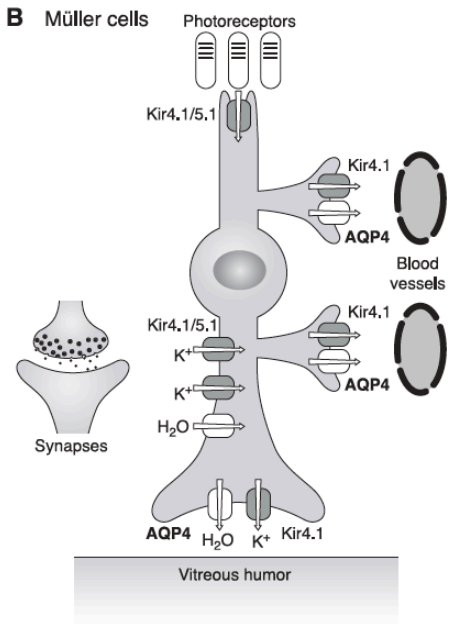

Figure 3-1 Retinal Müller cells express heteromeric Kir4.1/Kir5.1 channels at perisynaptic sites and homomeric Kir4.1 channels in perivascular processes and endfeet. The Kir4.1 channels coexist with the water channel AQP4 in the same membrane domain[20].

It is generally accepted that Kir4.1 channels are the predominant Kir channels in glial cell sand their function contributes to the resting conductance of astrocytes and Müller cells. A lack of Kir4.1 will cause irregular K^+ and glutamate homeostasis and glial membrane depolarization which finally leads to seizures in knockout mice[15]. Kir4.1 expression is up-regulated in cell culture and its function has been shown to be important in cell differentiation; its presence is correlated with an exit from the cell cycle[51].

Numerous studies have demonstrated that glial Kir4.1 expression and function decreases following acute injury and this is often associated with GFAP up-regulation and glial cell proliferation. In a rat model of experimental glaucoma, down regulation of K^+ currents was found, which was said to be due to Müller cell gliosis[52]. Kir4.1 channels are also associated with and co-localized with the water channel AQP4[53], the principle water

channel expressed in glial cells. However there is still controversy on the extent of co-dependence of Kir4.1 and AQP4. In this chapter, we will focus on the expression of Kir4.1 in macroglia in monkey retinas in eyes with experimental glaucoma. We will compare the findings in this chapter with the findings in the previous chapter on AQP4, to explore the potential role of Kir4.1 channels and water channels in retinal glia.

Methods

Animals

Four of the five rhesus monkeys whose retinas were studied in Chapter 2 were subjects for these experiments as well. For OHT-66, tissue was not available. The methods were the same as in the previous chapter except that for the immunohistochemistry, an antibody to Kir4.1 also was used (see Table 3-1)

Immunohistochemistry

The sections were exposed to rabbit anti-Kir4.1 antibody (1:100) and goat anti glial fibrillary acidic protein (GFAP) antibody (1:250) diluted in 1% normal donkey serum, 0.3% Triton X-100, 0.1% sodium azide in PBS overnight on a shaker at 4°C (Table. 2). All sections were washed with in PBS containing for 6*30 minutes, and then incubated with a Cy3-conjugated donkey anti-rabbit IgG (1:250) and Cy-5 conjugated donkey anti-goat IgG (1:250) diluted in PBS for 3 hours and were washed with PBS for 5*30 minutes[3]. The sections were put on to the slide and mounted in fluorescence mounting medium (Vector Vectashield H-1000)[44].

Table 3-1 Antibody List

Antigen	Host	Dilution	Source	Reference
Inward rectifier potassium channel 4.1 (Kir4.1)	Rabbit	1:125	Millipore, Billerica, MA, USA (AB5818-200UL)	--
Glial fibrillary acidic protein (GFAP)	Goat	1:250	AbCam, Cambridge, MA (Ab53554)	Bettum IJ et al., 2014
Cy™5 AffiniPure IgG (H+L)	Donkey anti-Goat IgG	1:250	Jackson ImmunoResearch (Code: 705-175-147)	--
Cy™3 AffiniPure F (ab')$_2$ Fragment IgG (H+L)	Donkey anti-Rabbit IgG	1:250	Jackson ImmunoResearch (Code: 711-166-152)	--

We first tried to identify Müller cell immunolabeling for Kir4.1 using the antibody against GS. However the Kir4.1 antibody appeared to compete with the GS antibody, causing unacceptably high background staining and little staining for either protein. We also tried to colocalize immunolabeling for Kir4.1 and Aquaporin 4 had similar problems. Therefore, we only used antibodies for localizing Kir4.1 and GFAP (astrocytes and reactivity in Müller cells). Sections from the same regions that were sampled for localizing AQP4 in normal monkey eyes and those with experimental glaucoma were used for Kir4.1 immunolabeling.

Results

Immunolabeling of Kir4.1 and glial marker in macaque monkey control eye

In Figure 3-2, retinas near the ONH (inferior region) of four monkeys were immunolabeled for Kir4.1 and for the astrocyte marker, GFAP. In the left column of

Figure 3-2, intense Kir4.1 labeling (red) was visible throughout the thickness of the control monkey retinas. Kir4.1 distribution was consistent with initial reports of Kir4.1 in isolated rat and rabbit retinal Müller cells[25], and later studies in mouse retina[20, 23]. Labeling was present in the OPL, in Müller cell processes in the INL, in the inner plexiform layer (IPL), surrounding retinal ganglion cells, in Müller cell trunks in the RNFL and in their endfeet. A similar distribution of Kir4.1 labeling was present in the superior region near the optic nerve head for the three monkeys,as shown in Figure 3-3, left column. GFAP labeling (blue) showed astrocytes primarily in the RNFL in both retinal regions as expected (Figure 3-2, 3-3, middle columns). To determine whether Kir4.1 was present in the astrocytes, the images labeled for Kir4.1 and GFAP were merged (Figure 3-2, 3-3, right column). In the merged images, the majority of the GFAP positive processes in the RNFL showed varied shades of purple, indicating that the amount of Kir4.1 was present in differing levels in the astrocytes (less in OHT-60 and 61, Figure 3-2, I and L).

Figure 3-2 and 3-3 near here

To find out whether experimental glaucoma altered Kir4.1 immunolabeling in the retina, we compared the control and experimental eyes, and results for the inferior region near the nerve head are shown in Figure 3-4 and Figure 3-5. In Figure 3-4, Kir4.1 labeling in experimental eyes was similar to that of control eyes for regions where Müller cells are present. Labeling for Kir4.1 was still present in the OPL, INL, and GCL. However, Kir4.1 immunoreactivity appeared to be increased in the region of the RNFL of both animals, and more so in the monkey with the more severe neuropathy, OCT-61 (47%, C, D). In Figure 3-5 (A, B) co-localized markers for Kir4.1 and GFAP in OHT-60 (40% loss

of RNFL) show Kir4.1 positive astrocytes in the remaining RNFL that are a little redder purple in places than they are it in control eyes (Figure 3-5 A, B) suggesting a small increase in Kir4.1 labeling. For the monkey with the more severe neuropathy OHT-61, Kir4.1 and GFAP labeling co-localized as purple and varied shades of fuchia in astrocytes of the nerve fiber layer and in the reactive GFAP positive regions of Müller cells.

Figure 3-4 and 3-5 near here

In the superior region of retina near the ONH for OHT-57 shown in Figure 3-5, the distribution of Kir4.1 in the experimental eye is similar to that seen in the control eye, but the labeling appears perhaps a little brighter. This region of the retina also showed signs of stress in the Müller cells (GFAP staining).

Discussion

Similarities

and differences in the distribution of Kir4.1 and AQP4 in the control eye, and in the changes that occur in the experimental eye.

In this portion of the present study, we found that Kir4.1 was distributed from OPL to RNFL in retinal regions near the optic nerve head both in the normal monkey eyes and in eyes with experimental glaucoma. Although we tried to remove high background staining for Kir4.1 by eliminating the GS antibody, the results still showed widespread staining for Kir4.1. The reason for this is not clear. It is encouraging, however, that the brightest labeling for Kir4.1 was in regions where Müller cells are known to be present, e.g. in the OPL and through the INL, around ganglion cells, and trunks around nerve fiber bundles.

Although the regional variations in the intensity of the labeling for Kir4.1 were not as great as they were for AQP4 in Chapter 2, the labels for the two antibodies were in similar locations, and these locations were confirmed to be co-localized with GS, a Muller cell marker, in Chapter 2. The similarities in distribution of AQP4 and Kir4.1 labeling in the control eye can be seen in Figure 3-7 A and B where labeling is shown for Monkey OHT-61 for AQP4 (and GFAP) on the left , and labeling for Kir4.1 (and GFAP) on the right

Although Figure 3-7 and previous figures in the thesis, confirm labeling for both AQP4 and Kir4.1 in the Müller cells in control eyes, the distribution of the two different channels did not change in the same way in experimental glaucoma. The decrease in AQP4 labeling that we observed in Müller cells was not paralleled by a similar decrease for Kir4.1. In Figure 3-7 although the labeling pattern for the AQP4 and GFAP is quite similar in the control eye of OHT-61, the pattern of labeling for the two protein channels is much less similar in the experimental eye (C and D), where AQP4 labeling is dramatically decreased in the Müller cells, but labeling for Kir4.1, appears to be unaltered from control in all layers except the RNFL.

Our findings in Chapter 2 suggested altered expression of AQP4 in the astrocytes of the RNFL, small increases during the early stages of neuropathy, and progressively enhanced expression with increasing axonal loss (Figure 2.7). That enhancement is clear for AQP4 in OHT-61 (47% RNFL loss) in Figure 3.4 and again in Figure 3-7 where the RNFL region in the experimental eye is dense with an aqua color due to co-localization of AQP4 and GFAP, whereas the control eye (Figure 3-7 A) shows only wisps of blue. The

aggregation of the astrocytes themselves in the experimental eye is more clearly seen in Figure 3-8 where labeling for GFAP is shown alone for these retinal sections.

In the results for Kir4.1 in Chapter 3, findings in some eyes were consistent with enhanced expression of Kir4.1, as well, in the region of the nerve fiber layer in the experimental eye. In particular increased labeling for Kir4.1 can be seen in Figure 3.4 (A,B) in the experimental eye of OHT-60 to some extent, and to a much larger extent in OHT-61 (Figure 3.4, C,D) . For OHT-61 (Figure 3.7) the label for Kir4.1 co-localized with the label for GFAP in aggregated astrocytes to about the same extent that the label for AQP4 co-localized with the label for GFAP (also see Figure 3-8 for GFAP labeling alone).

Related activity of Kir4.1 and AQP4 channels

As reviewed in the Introduction to this thesis, spatial co-localization of AQP4 and Kir4.1 channels on the endfeet processes of the Müller cells facing the vitreous and blood vessels of the mammalian retina has been described, and it has been suggested that the two channels work together to facilitate water transport across membranes when there are differences in osmotic gradients or hydrostatic pressure inside and outside of cells. [11] Nagelhus et al[53] reported co-localization of Kir4.1 channels and AQP4 channels in immunogold-EM sections. There also are some disagreements about co-dependence of AQP4 and Kir4.1 in glia. For example, in a study of AQP4 knockout mice, freshly isolated Müller cells did not show changes in Kir4.1 protein expression[54] that might have been expected if they are related, and in a study in the brain, there was no significant difference in water permeability with inhibition of Kir4.1 channels[55]. However, this independence in the development and function of the channels does not preclude effects

on the function of the other channel's function in glial cells if the presence of one type of channel is decreased. A loss of AQP4 channels in Müller cells could disrupt Müller cell K^+ currents, due to changes in osmotic gradients and as a consequence, reduce the driving force for moving K^+ from the extracellular space into Müller cells via Kir4.1 channels. Our ERG studies in the experimental glaucoma model raise the possibility of a disruption of K^+ spatial buffer currents[27, 41], and it is possible that this alteration is due to the loss of AQP4 in Müller cells. Although Kir 4.1 channels appear to remain in Müller cells in experimental eyes, but they may not function normally.

Further considerations, future studies

It has been reported in diabetic rats[55] that when AQP4 was lost from Müller cells during neurodegeneration, another aquaporin, AQP1, not normally associated with Müller cells was detected in those cells. It will be important to label for AQP1and perhaps other aquaporins in the macaque experimental glaucoma model to see if other aquaporins are present in the experimental (and control) eye. It will also be important to follow the fate in macaque experimental glaucoma of AQP9, an aquaporin normally found in retinal ganglion cells, and affected in experimental glaucoma in rodents.[3, 16] Similarly for Kir4.1, different Kir channels may also be involved in spatial buffering and affected in experimental glaucoma. Kir4.1 has been reported to be both homomeric and heteromeric (with Kir2.1 or Kir5.1) by Butt et al[30] in CNS glia, and (with Kir5.1 in rat Müller cells by Ishii et al[50]f. If Kir4.1 is heteromeric in Müller cells in monkeys, stronger regional distribution could be present for certain combinations of Kir channel types in normal eyes than was seen for Kir4.1 alone in the present study, and changes could occur in the heteromeric channels in the experimental eye that were not detected in our experiments.

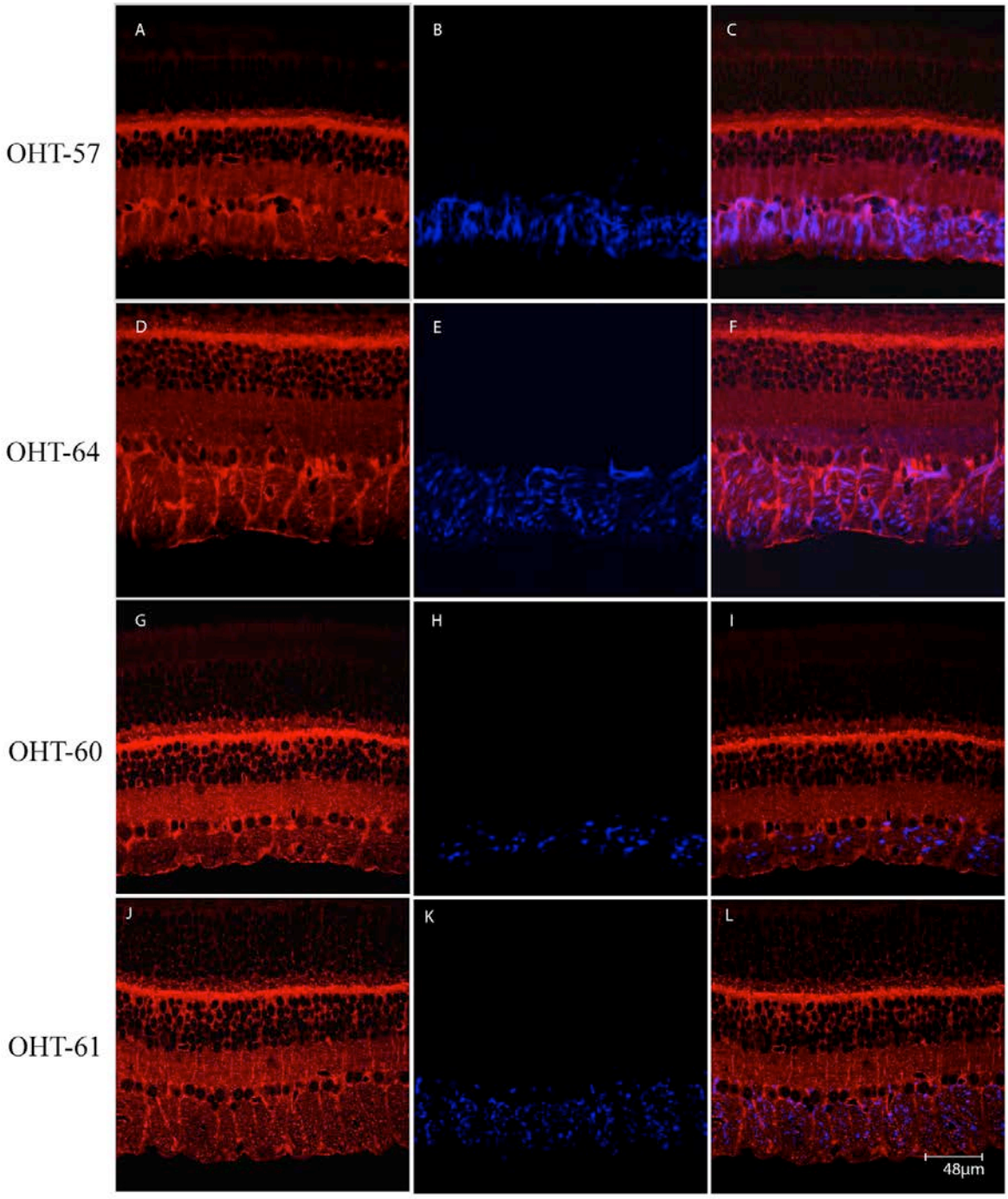

Figure 3-2 Immunolabeling for Kir4.1 and GFAP in the control retina within 5 mm of the ONH, inferior region for four monkeys (OHT-57, OHT-64, OHT-60 and OHT-61). Left column A, D, G, J: single labeling of Kir4.1. Middle column B, E, H, K: single labeling of GFAP. Right column C, F, I, L: double labeling of Kir4.1 and GFAP.

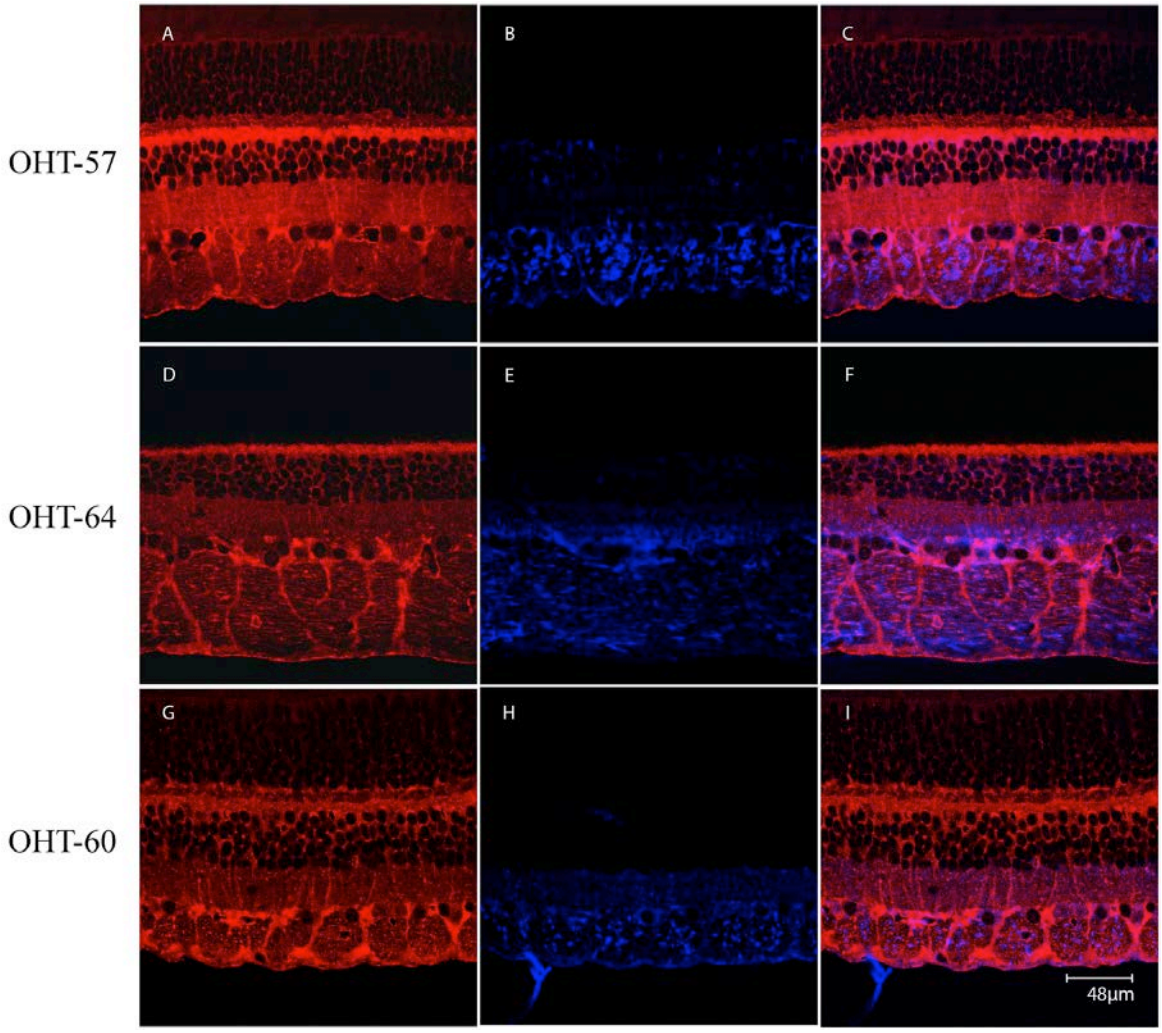

Figure 3-3 Immunolabeling for Kir4.1 and GFAP in the control retina within 5 mm of the ONH, superior region, for three monkeys (OHT-57, OHT-64, OHT-60). (Images for all are 63x Zoom 1x, 1 section projection, 0.5µm) Left column A, D, G: single labeling of Kir4.1. Middle column B, E, H: single labeling of GFAP. Right column C, F, I: double labeling of Kir4.1 and GFAP.

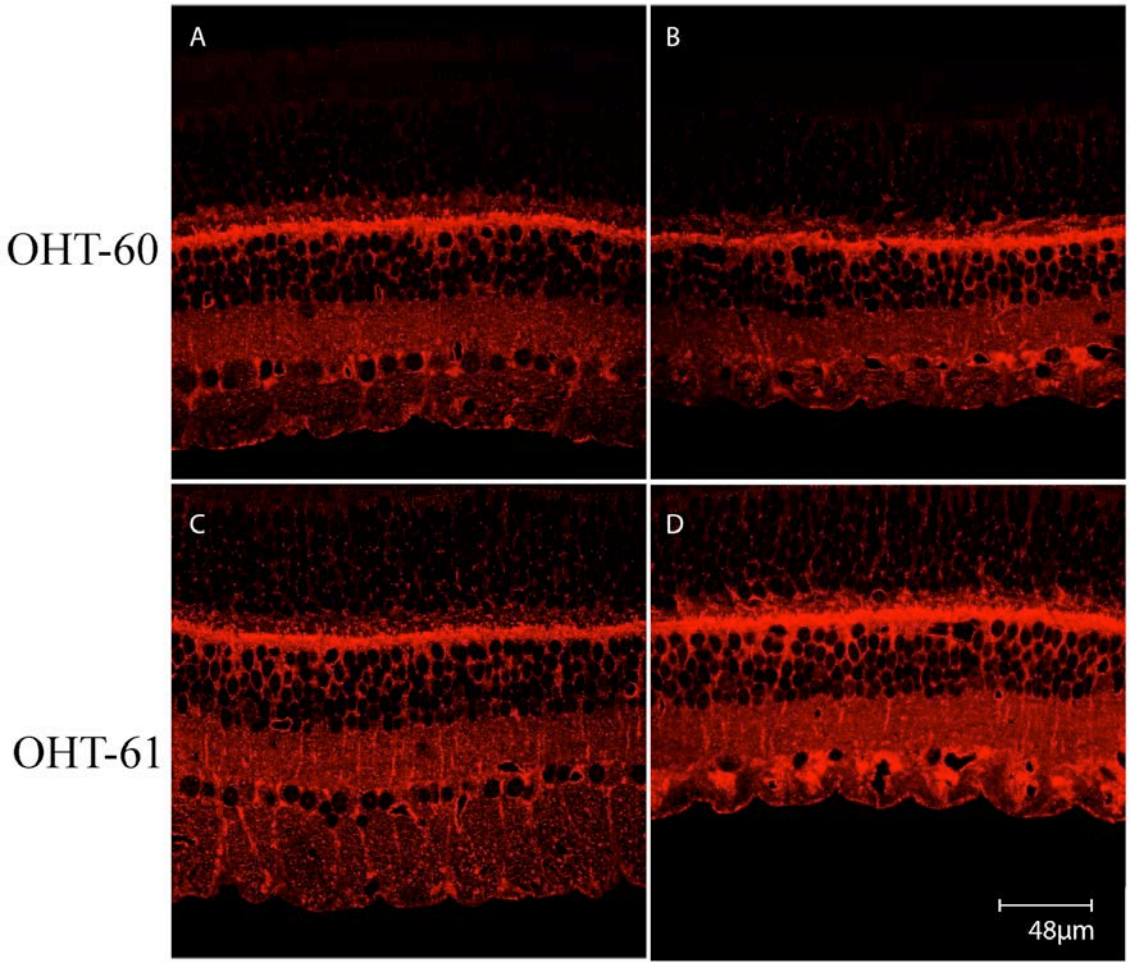

Figure 3-4 Immunolabeling for Kir4.1 in the control and experimental retina within 5 mm of the optic nerve head, inferior region for two monkeys (OHT-60 and OHT-61). (Images are 63x Zoom 1x, 1 section projection, 0.5µm). The relative nerve fiber layer loss increased from top to bottom. The left column (A, C) shows the control eye, the right column (C, D) shows the experimental glaucoma eye.

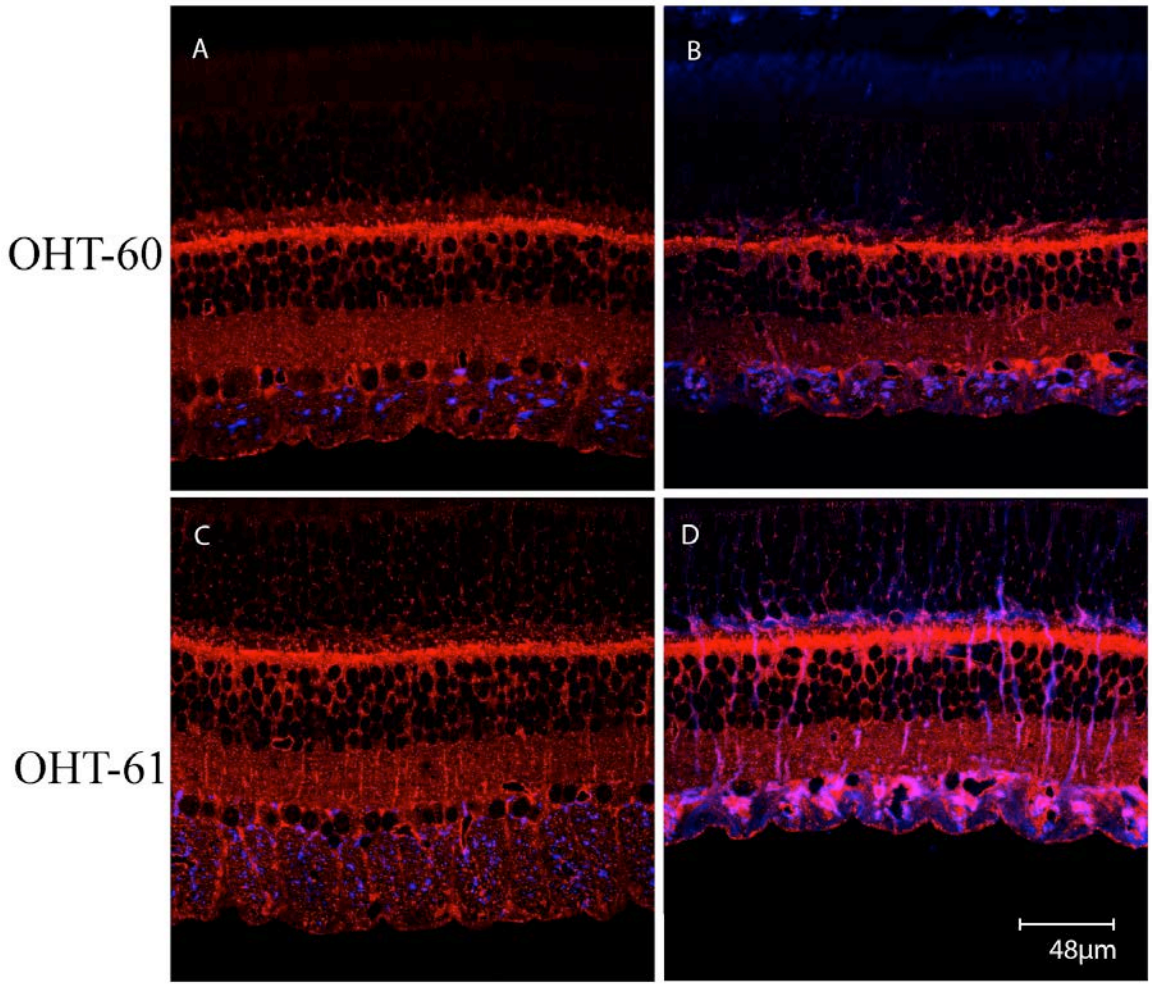

Figure 3-5 Double immunolabeling for Kir4.1 and GFAP in the control and experimental retina within 5 mm of the optic nerve head, inferior region for two monkeys (OHT-60 and OHT-61). (Images are 63x Zoom 1x, 1 section projection, 0.5µm). The relative nerve fiber layer loss increased from top to bottom. The left column (A, C) shows the control eye, the right column (C, D) shows the experimental glaucoma eye.

OHT-57

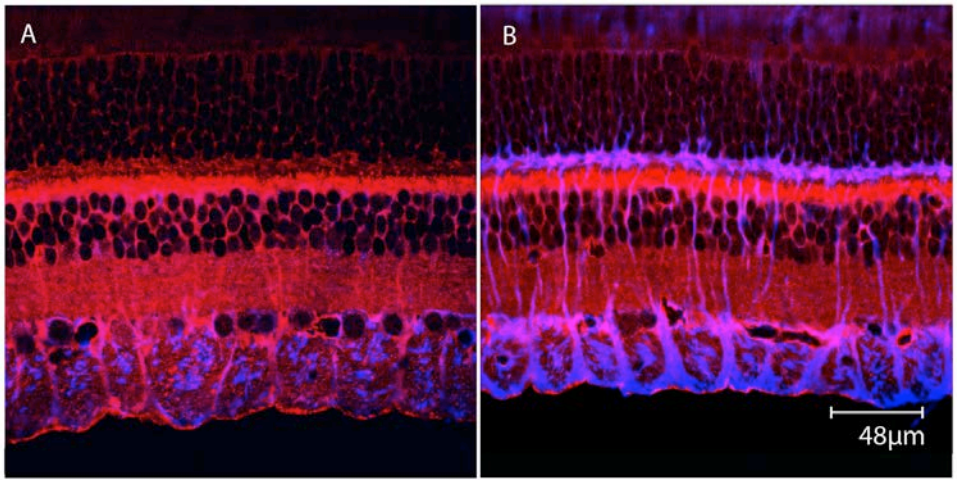

Figure 3-6 Double immunolabeling of Kir4.1 and GFAP in the control and experimental retina within 5 mm of the optic nerve head, superior region for one monkey, OHT-57. (Images are 63x Zoom 1x, 1 section projection, 0.5µm). Image A shows the control eye, Image B shows the experimental glaucoma eye.

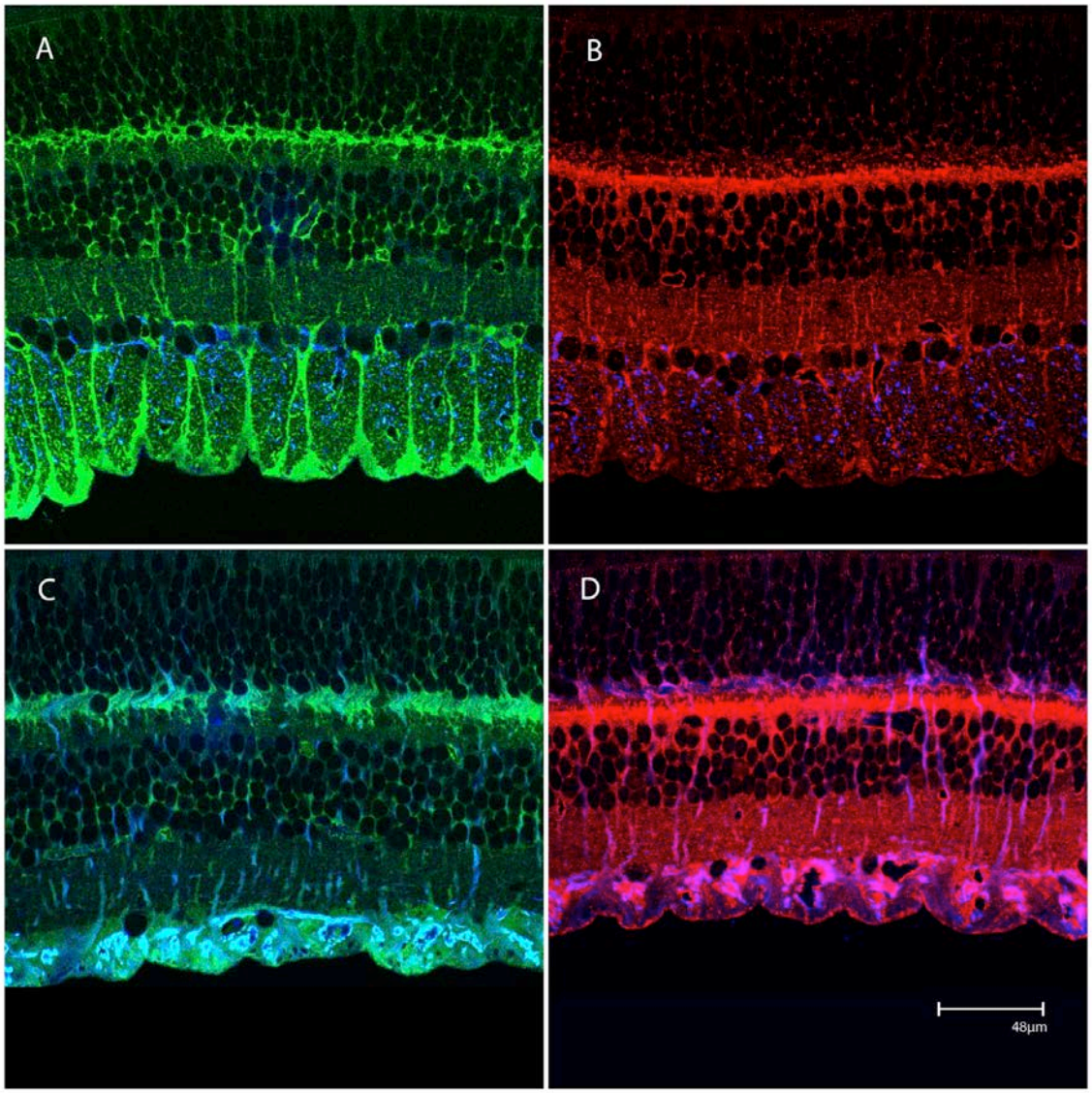

Figure 3-7 Double immunolabeling for AQP4 and GFAP (A, C), and for Kir4.1 and GFAP (B, D) for the control retina (A, B) and the experimental retina (C, D) within 5 mm of the ONH, inferior region for monkey OHT-61. (Images are 63x Zoom 1x, 1 section projection, 0.5 µm.)

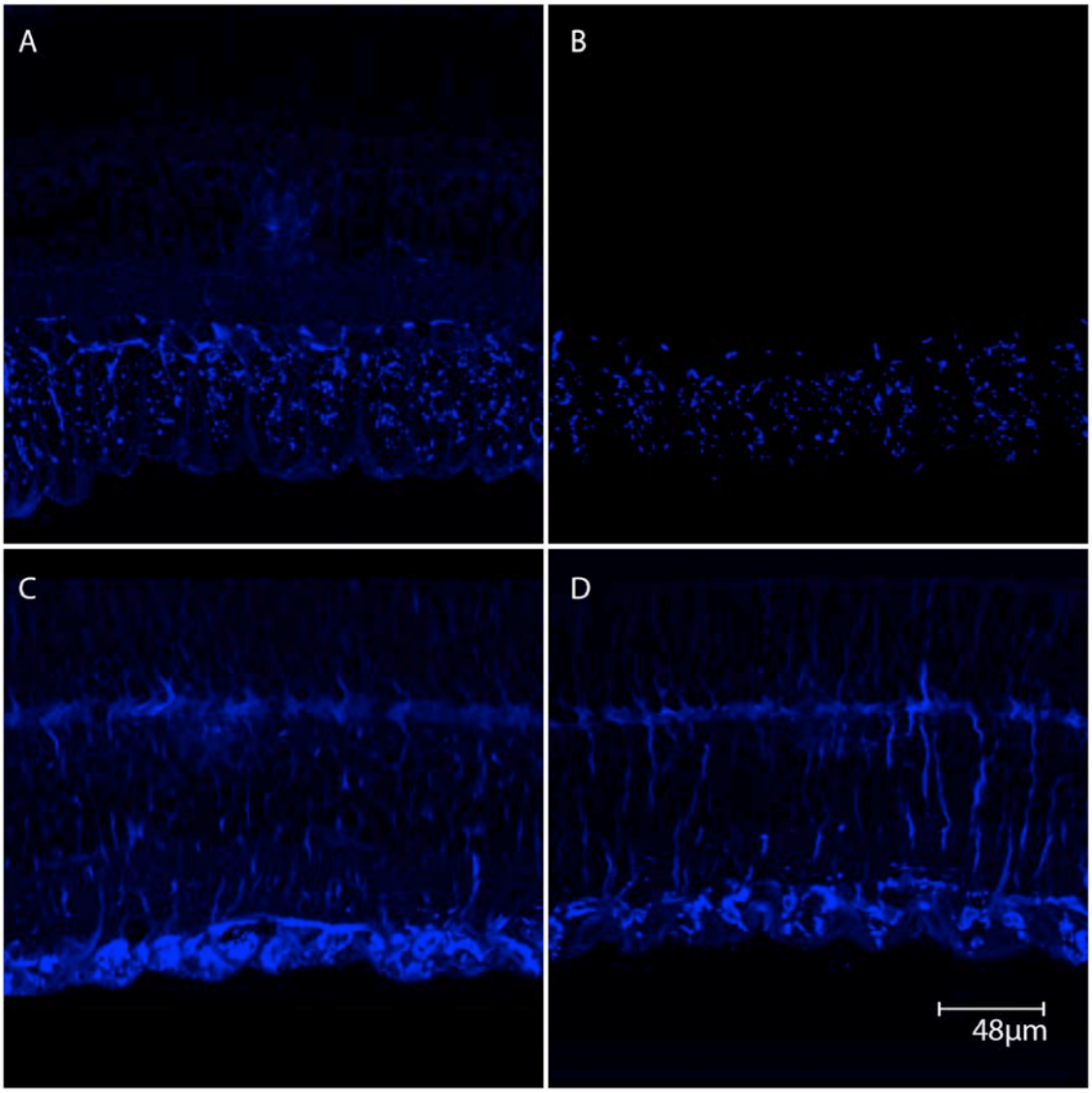

Figure 3-8 Immunolabeling for GFAP alone (same sections as in Figure 3-6) for the control retina (A, B) and the experimental retina (C, D) within 5 mm of the ONH, inferior region for monkey OHT-61. (Images are 63x Zoom 1x, 1 section projection, 0.5µm.)

References

1. Schey KL, Wang Z, J LW, Qi Y. Aquaporins in the eye: expression, function, and roles in ocular disease. *Biochim Biophys Acta* 2014;1840:1513-1523.

2. Fischbarg J. Water channels and their roles in some ocular tissues. *Mol Aspects Med* 2012;33:638-641.

3. Dibas A, Yang MH, He S, Bobich J, Yorio T. Changes in ocular aquaporin-4 (AQP4) expression following retinal injury. *Mol Vis* 2008;14:1770-1783.

4. Verkman AS. Role of aquaporin water channels in eye function. *Exp Eye Res* 2003;76:137-143.

5. Otterbach F, Callies R, Adamzik M, et al. Aquaporin 1 (AQP1) expression is a novel characteristic feature of a particularly aggressive subgroup of basal-like breast carcinomas. *Breast Cancer Res Treat* 2010;120:67-76.

6. Watanabe T, Fujii T, Oya T, et al. Involvement of aquaporin-5 in differentiation of human gastric cancer cells. *J Physiol Sci* 2009;59:113-122.

7. Garfias Y, Navas A, Perez-Cano HJ, Quevedo J, Villalvazo L, Zenteno JC. Comparative expression analysis of aquaporin-5 (AQP5) in keratoconic and healthy corneas. *Mol Vis* 2008;14:756-761.

8. Kenney MC, Atilano SR, Zorapapel N, Holguin B, Gaster RN, Ljubimov AV. Altered expression of aquaporins in bullous keratopathy and Fuchs' dystrophy corneas. *J Histochem Cytochem* 2004;52:1341-1350.

9. Papadopoulos MC, Verkman AS. Aquaporin water channels in the nervous system. *Nat Rev Neurosci* 2013;14:265-277.

10. Nagelhus EA, Veruki ML, Torp R, et al. Aquaporin-4 water channel protein in the rat retina and optic nerve: polarized expression in Muller cells and fibrous astrocytes. *J Neurosci* 1998;18:2506-2519.

11. Nagelhus EA, Mathiisen TM, Ottersen OP. Aquaporin-4 in the central nervous system: cellular and subcellular distribution and coexpression with KIR4.1. *Neuroscience* 2004;129:905-913.

12. Feng X, Papadopoulos MC, Liu J, et al. Sporadic obstructive hydrocephalus in Aqp4 null mice. *J Neurosci Res* 2009;87:1150-1155.

13. Da T, Verkman AS. Aquaporin-4 gene disruption in mice protects against impaired retinal function and cell death after ischemia. *Invest Ophthalmol Vis Sci* 2004;45:4477-4483.

14. Amiry-Moghaddam M, Williamson A, Palomba M, et al. Delayed K+ clearance associated with aquaporin-4 mislocalization: phenotypic defects in brains of alpha-syntrophin-null mice. *Proc Natl Acad Sci U S A* 2003;100:13615-13620.

15. Binder DK, Oshio K, Ma T, Verkman AS, Manley GT. Increased seizure threshold in mice lacking aquaporin-4 water channels. *Neuroreport* 2004;15:259-262.

16. Yang MH, Dibas A, Tyan YC. Changes in retinal aquaporin-9 (AQP9) expression in glaucoma. *Biosci Rep* 2013;33.

17. Tran TL, Bek T, la Cour M, et al. Altered aquaporin expression in glaucoma eyes. *APMIS* 2014;122:772-780.

18. Hernandez MR. The optic nerve head in glaucoma: role of astrocytes in tissue remodeling. *Prog Retin Eye Res* 2000;19:297-321.

19. Verkman AS, Binder DK, Bloch O, Auguste K, Papadopoulos MC. Three distinct roles of aquaporin-4 in brain function revealed by knockout mice. *Biochim Biophys Acta* 2006;1758:1085-1093.

20. Hibino H, Inanobe A, Furutani K, Murakami S, Findlay I, Kurachi Y. Inwardly rectifying potassium channels: their structure, function, and physiological roles. *Physiol Rev* 2010;90:291-366.

21. Kofuji P, Ceelen P, Zahs KR, Surbeck LW, Lester HA, Newman EA. Genetic inactivation of an inwardly rectifying potassium channel (Kir4.1 subunit) in mice: phenotypic impact in retina. *J Neurosci* 2000;20:5733-5740.

22. Newman EA. Regional specialization of retinal glial cell membrane. *Nature* 1984;309:155-157.

23. Newman EA. Voltage-dependent calcium and potassium channels in retinal glial cells. *Nature* 1985;317:809-811.

24. Kofuji P, Biedermann B, Siddharthan V, et al. Kir potassium channel subunit expression in retinal glial cells: implications for spatial potassium buffering. *Glia* 2002;39:292-303.

25. Ishii M, Horio Y, Tada Y, et al. Expression and clustered distribution of an inwardly rectifying potassium channel, KAB-2/Kir4.1, on mammalian retinal Muller cell membrane: their regulation by insulin and laminin signals. *J Neurosci* 1997;17:7725-7735.

26. Colotto A, Falsini B, Salgarello T, Iarossi G, Galan ME, Scullica L. Photopic negative response of the human ERG: losses associated with glaucomatous damage. *Invest Ophthalmol Vis Sci* 2000;41:2205-2211.

27. Viswanathan S, Frishman LJ, Robson JG, Harwerth RS, Smith EL, 3rd. The photopic negative response of the macaque electroretinogram: reduction by experimental glaucoma. *Invest Ophthalmol Vis Sci* 1999;40:1124-1136.

28. Frishman LJ, Steinberg RH. Light-evoked increases in [K+]o in proximal portion of the dark-adapted cat retina. *J Neurophysiol* 1989;61:1233-1243.

29. Thompson DA, Feather S, Stanescu HC, et al. Altered electroretinograms in patients with KCNJ10 mutations and EAST syndrome. *J Physiol* 2011;589:1681-1689.

30. Butt AM, Kalsi A. Inwardly rectifying potassium channels (Kir) in central nervous system glia: a special role for Kir4.1 in glial functions. *J Cell Mol Med* 2006;10:33-44.

31. Yang Z, Huang P, Liu X, et al. Effect of adenosine and adenosine receptor antagonist on Muller cell potassium channel in Rat chronic ocular hypertension models. *Sci Rep* 2015;5:11294.

32. Iandiev I, Tenckhoff S, Pannicke T, et al. Differential regulation of Kir4.1 and Kir2.1 expression in the ischemic rat retina. *Neurosci Lett* 2006;396:97-101.

33. Iandiev I, Pannicke T, Hollborn M, et al. Localization of glial aquaporin-4 and Kir4.1 in the light-injured murine retina. *Neurosci Lett* 2008;434:317-321.

34. Bataveljic D, Nikolic L, Milosevic M, Todorovic N, Andjus PR. Changes in the astrocytic aquaporin-4 and inwardly rectifying potassium channel expression in the brain of the amyotrophic lateral sclerosis SOD1(G93A) rat model. *Glia* 2012;60:1991-2003.

35. Distler C, Weigel H, Hoffmann KP. Glia cells of the monkey retina. I. Astrocytes. *J Comp Neurol* 1993;333:134-147.

36. Distler C, Dreher Z. Glia cells of the monkey retina--II. Muller cells. *Vision Res* 1996;36:2381-2394.

37. Varela HJ, Hernandez MR. Astrocyte responses in human optic nerve head with primary open-angle glaucoma. *J Glaucoma* 1997;6:303-313.

38. Seitz R, Ohlmann A, Tamm ER. The role of Muller glia and microglia in glaucoma. *Cell Tissue Res* 2013;353:339-345.

39. Shields M. The Optic Nerve Head. Textbook of Glaucoma. Philadelphia, PA: Williams & Wilkins; 1987.

40. Larsen BR, MacAulay N. Kir4.1-mediated spatial buffering of K(+): experimental challenges in determination of its temporal and quantitative contribution to K(+) clearance in the brain. *Channels (Austin)* 2014;8:544-550.

41. Luo X, Patel NB, Rajagopalan LP, Harwerth RS, Frishman LJ. Relation between macular retinal ganglion cell/inner plexiform layer thickness and multifocal electroretinogram measures in experimental glaucoma. *Invest Ophthalmol Vis Sci* 2014;55:4512-4524.

42. Quigley HA, Hohman RM. Laser energy levels for trabecular meshwork damage in the primate eye. *Invest Ophthalmol Vis Sci* 1983;24:1305-1307.

43. Harwerth RS, Smith EL, 3rd, DeSantis L. Behavioral perimetry in monkeys. *Invest Ophthalmol Vis Sci* 1993;34:31-40.

44. Carter-Dawson L, Zhang Y, Harwerth RS, et al. Elevated albumin in retinas of monkeys with experimental glaucoma. *Invest Ophthalmol Vis Sci* 2010;51:952-959.

45. Nagelhus EA, Ottersen OP. Physiological roles of aquaporin-4 in brain. *Physiol Rev* 2013;93:1543-1562.

46. Chen CT, Alyahya K, Gionfriddo JR, Dubielzig RR, Madl JE. Loss of glutamine synthetase immunoreactivity from the retina in canine primary glaucoma. *Vet Ophthalmol* 2008;11:150-157.

47. Nagelhus EA, Lehmann A, Ottersen OP. Neuronal-glial exchange of taurine during hypo-osmotic stress: a combined immunocytochemical and biochemical analysis in rat cerebellar cortex. *Neuroscience* 1993;54:615-631.

48. Mizokami J, Kanamori A, Negi A, Nakamura M. A preliminary study of reduced expression of aquaporin-9 in the optic nerve of primate and human eyes with glaucoma. *Curr Eye Res* 2011;36:1064-1067.

49. Djukic B, Casper KB, Philpot BD, Chin LS, McCarthy KD. Conditional knock-out of Kir4.1 leads to glial membrane depolarization, inhibition of potassium and glutamate uptake, and enhanced short-term synaptic potentiation. *J Neurosci* 2007;27:11354-11365.

50. Ishii M, Fujita A, Iwai K, et al. Differential expression and distribution of Kir5.1 and Kir4.1 inwardly rectifying K+ channels in retina. *Am J Physiol Cell Physiol* 2003;285:C260-267.

51. Olsen ML, Sontheimer H. Functional implications for Kir4.1 channels in glial biology: from K+ buffering to cell differentiation. *J Neurochem* 2008;107:589-601.

52. Ji M, Miao Y, Dong LD, et al. Group I mGluR-mediated inhibition of Kir channels contributes to retinal Muller cell gliosis in a rat chronic ocular hypertension model. *J Neurosci* 2012;32:12744-12755.

53. Nagelhus EA, Horio Y, Inanobe A, et al. Immunogold evidence suggests that coupling of K+ siphoning and water transport in rat retinal Muller cells is mediated by a coenrichment of Kir4.1 and AQP4 in specific membrane domains. *Glia* 1999;26:47-54.

54. Ruiz-Ederra J, Zhang H, Verkman A. Evidence against functional interaction between aquaporin-4 water channels and Kir4. 1 potassium channels in retinal Müller cells. *Journal of Biological Chemistry* 2007;282:21866-21872.

55. Zhang H, Verkman AS. Aquaporin-4 independent Kir4.1 K+ channel function in brain glial cells. *Mol Cell Neurosci* 2008;37:1-10.

APPENDIX

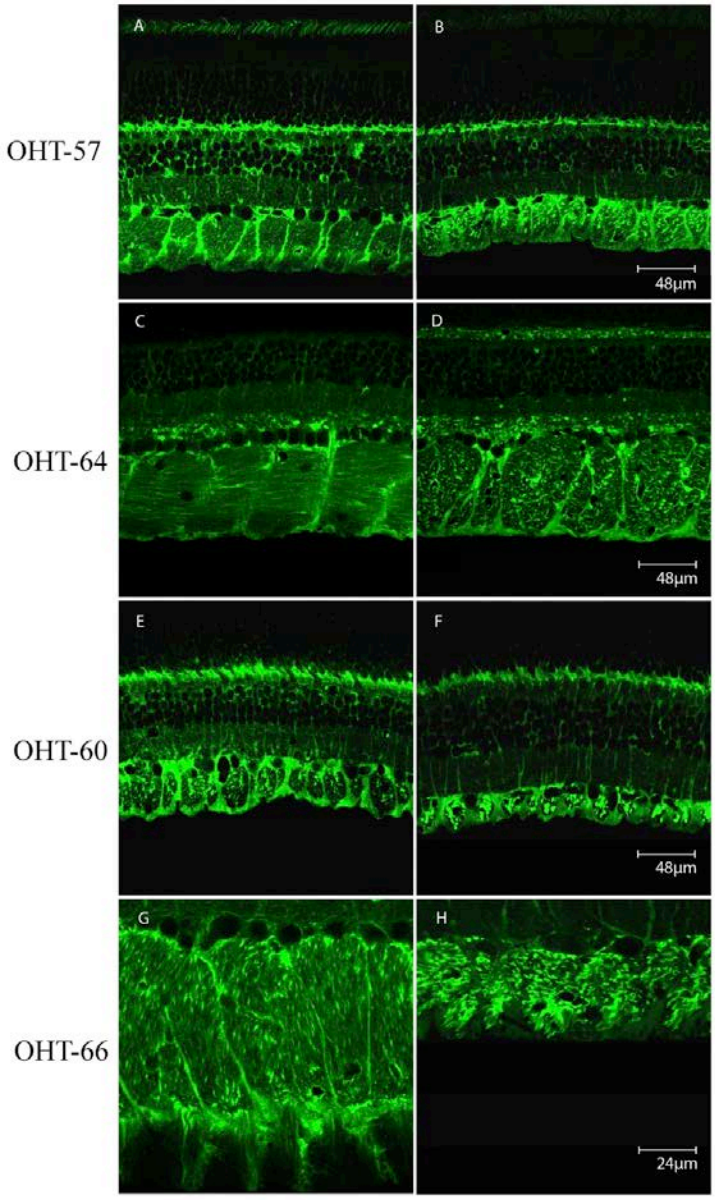

Appendix Figure 1 Immunolabeling for AQP4 of the retina within 5 mm of the OHN in the superior region for control and experimental eyes of four monkeys (OHT-57, OHT-64, OHT-60 and OHT-66). (Images for OHT-57, OHT-64 and OHT-60 are 63x Zoom 1x, 1 section projection, 0.5µm. Images for OHT-66 are 63x Zoom 2x, 1 section projection, 0.5µm) From top to bottom, the relative nerve fiber loss increased. The left column (A, C, E, G) shows the control eye, the right column (B, D, F, H) shows the experimental glaucoma eye.

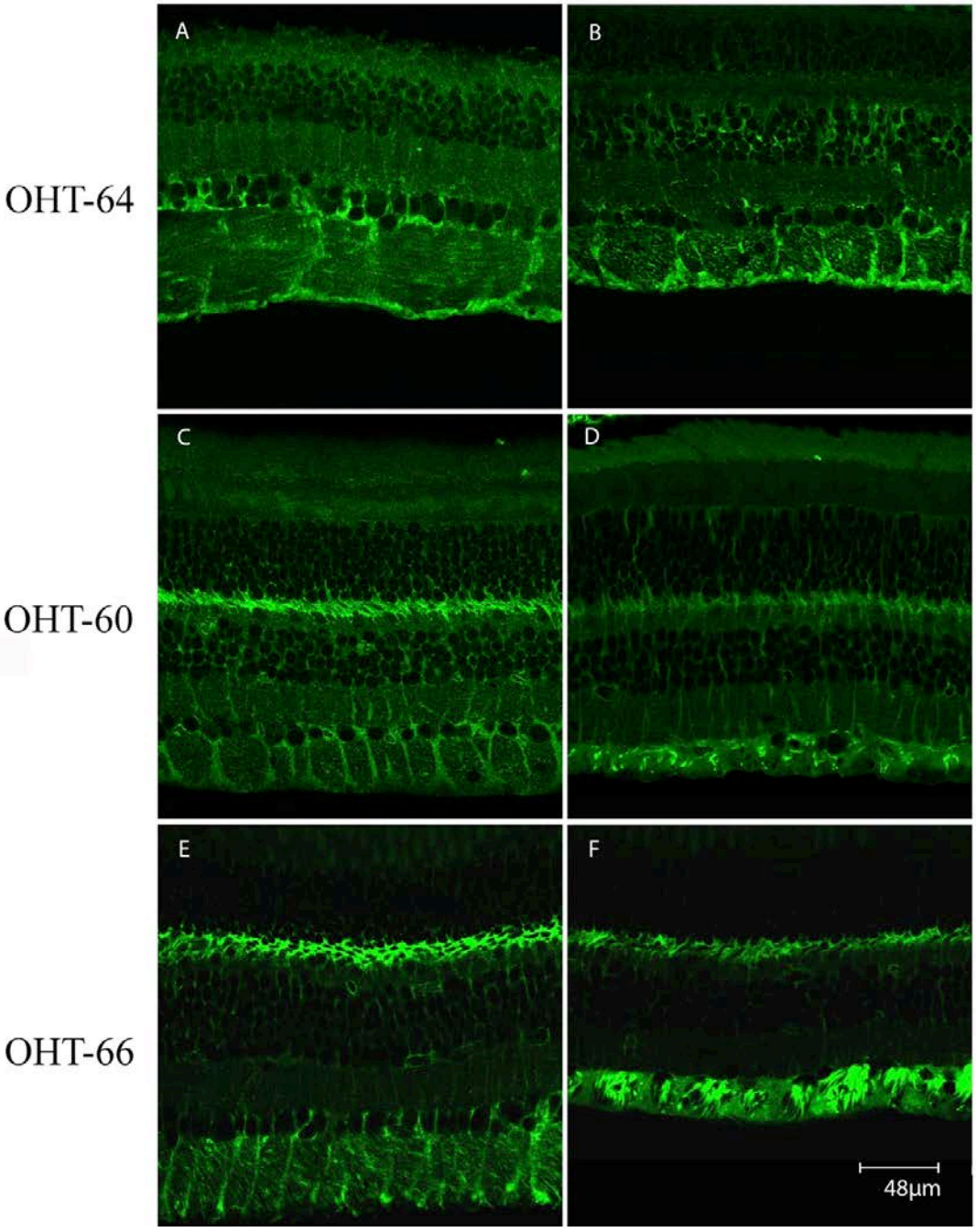

Appendix Figure 2 Immunolabeling for AQP4 in the retina within 5 mm of the ONH nasal region in the control eye and experimental eyes of three monkeys (OHT-64, OHT-60 and OHT-66) in nasal region. (Images for all are 63x Zoom 1x, 1 section projection) From top to bottom, the nerve fiber loss increased. The left column (A, C, E) shows the control eye, the right column (B, D, F) shows the experimental glaucoma eye.